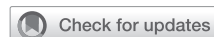
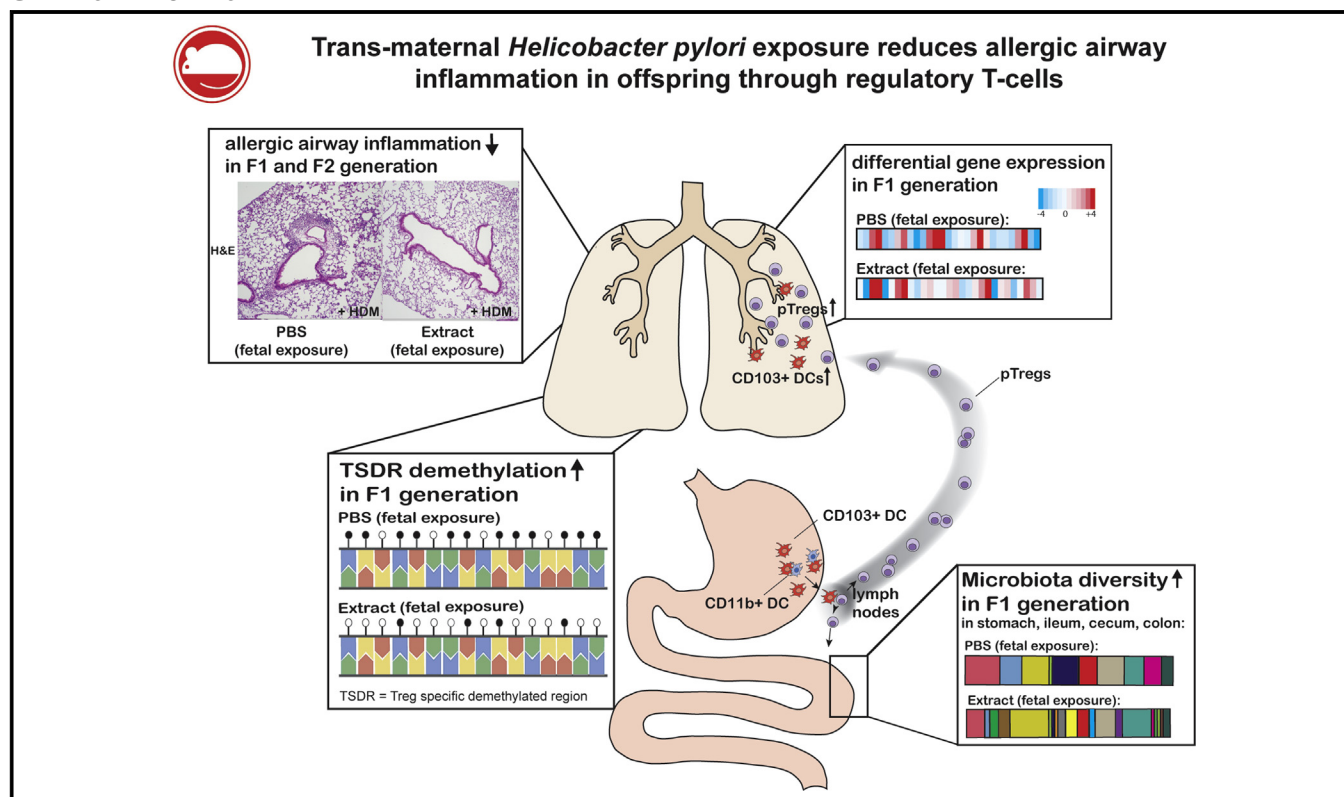


# Transmaternal *Helicobacter pylori* exposure reduces allergic airway inflammation in offspring through regulatory T cells



Andreas Kyburz, PhD,<sup>a</sup> Angela Fallegger, MSc,<sup>a</sup> Xiaozhou Zhang, MSc,<sup>a</sup> Aleksandra Altobelli, MSc,<sup>a</sup> Mariela Artola-Boran, MSc,<sup>a</sup> Timothy Borbet, MSc,<sup>b</sup> Sabine Urban, PhD,<sup>a</sup> Petra Paul, PhD,<sup>c</sup> Christian Münz, MD,<sup>c</sup> Stefan Floess, PhD,<sup>d</sup> Jochen Huehn, PhD,<sup>d</sup> Timothy L. Cover, MD,<sup>e</sup> Martin J. Blaser, MD,<sup>b</sup> Christian Taube, MD,<sup>f</sup> and Anne Müller, PhD<sup>a</sup> Zurich, Switzerland, New York, NY, Braunschweig and Essen, Germany, and Nashville, Tenn

## GRAPHICAL ABSTRACT



**Background:** Transmaternal exposure to tobacco, microbes, nutrients, and other environmental factors shapes the fetal immune system through epigenetic processes. The gastric microbe *Helicobacter pylori* represents an ancestral

constituent of the human microbiota that causes gastric disorders on the one hand and is inversely associated with allergies and chronic inflammatory conditions on the other.

From <sup>a</sup>the Institute of Molecular Cancer Research and <sup>c</sup>the Institute of Experimental Immunology, University of Zürich; <sup>b</sup>the Human Microbiome Program, New York University Langone Medical Center, New York; <sup>d</sup>the Department Experimental Immunology, Helmholtz Centre for Infection Research, Braunschweig; <sup>e</sup>Vanderbilt University Medical Center and Veterans Affairs Tennessee Valley Healthcare System, Nashville; and <sup>f</sup>the Department of Pulmonary Medicine, University Hospital Essen-Ruhrlandklinik, Essen.

Supported by the Swiss National Science Foundation Temporary Backup Schemes Consolidator Grant BSCGIO\_157841/1 and the Clinical Research Priority Program on Human Hemato-Lymphatic Diseases, University of Zurich (both to A.M.). Additional funds were supplied by the National Institutes of Health (grants AI039657 and CA116087) and Department of Veterans Affairs BX000627 (all to T.L.C.), as well as the Swiss National Science Foundation (project grant 310030\_162560 to C.M.). P.P. is supported by HFSP (LT000438/2014) and Marie Curie Fellowships (PIEF-GA-2013-623055). We further acknowledge National Institutes of Health support (U01AI22285 to M.J.B.), training grant support

(TL1TR001447 to T.B.), the NYUMC Genome Technology Center for sequencing assistance (partially supported by P30CA016087), and support through the C&D fund. Disclosure of potential conflict of interest: The authors declare that they have no relevant conflicts of interest.

Received for publication April 10, 2018; revised June 29, 2018; accepted for publication July 20, 2018.

Available online September 19, 2018.

Corresponding author: Anne Müller, PhD, Institute of Molecular Cancer Research, University of Zürich, Winterthurerstr 190, 8057 Zürich, Switzerland. E-mail: [mueллер@imcr.uzh.ch](mailto:mueллер@imcr.uzh.ch).

The CrossMark symbol notifies online readers when updates have been made to the article such as errata or minor corrections

0091-6749/\$36.00

© 2018 American Academy of Allergy, Asthma & Immunology

<https://doi.org/10.1016/j.jaci.2018.07.046>

**Objective:** Here we investigate the consequences of transmaternal exposure to *H pylori in utero* and/or during lactation for susceptibility to viral and bacterial infection, predisposition to allergic airway inflammation, and development of immune cell populations in the lungs and lymphoid organs.

**Methods:** We use experimental models of house dust mite– or ovalbumin-induced airway inflammation and influenza A virus or *Citrobacter rodentium* infection along with metagenomics analyses, multicolor flow cytometry, and bisulfite

pyrosequencing, to study the effects of *H pylori* on allergy severity and immunologic and microbiome correlates thereof.

**Results:** Perinatal exposure to *H pylori* extract or its immunomodulator vacuolating cytotoxin confers robust protective effects against allergic airway inflammation not only in first- but also second-generation offspring but does not increase susceptibility to viral or bacterial infection. Immune correlates of allergy protection include skewing of regulatory over effector T cells, expansion of regulatory T-cell subsets expressing CXCR3 or retinoic acid–related orphan receptor  $\gamma$ t, and demethylation of the forkhead box P3 (*FOXP3*) locus. The composition and diversity of the gastrointestinal microbiota is measurably affected by perinatal *H pylori* exposure.

**Conclusion:** We conclude that exposure to *H pylori* has consequences not only for the carrier but also for subsequent generations that can be exploited for interventional purposes. (*J Allergy Clin Immunol* 2019;143:1496-512.)

**Key words:** Allergic airway inflammation, microbial interventions during pregnancy, immune regulation, immune tolerance, metagenomics, epigenetic regulation of allergy and asthma

The prevalence of allergic asthma has increased dramatically in recent decades, with approximately 235 million persons affected worldwide.<sup>1</sup> Environmental and lifestyle factors that include diet, exposure to antibiotics, sanitary conditions, country of birth, exposure to pets and livestock, delivery mode, and breastfeeding, sometimes collectively referred to as the “exposome,” have all been causally implicated in this trend.<sup>2,3</sup> Many of the environmental factors affecting asthma and allergy risk act early in life (ie, leave their strongest marks on young adults, children, newborns, and even the unborn fetus).<sup>2,3</sup> Others act not only on the exposed subject but can manifest in subsequent generations. Examples of environmental factors that preferentially or exclusively act early in life include exposure to rural farming environments and livestock, which decreases the atopic sensitization and allergy risk of (directly exposed) children and the offspring of exposed pregnant mothers through mechanisms that appear to involve regulatory T (Treg) cells.<sup>4,5</sup> Other factors contributing to allergy risk early in life are the mode of birth (ie, vaginal or caesarean section delivery), as well as breastfeeding, which affect the establishment of a diverse human gut microbiota; recent studies suggest that microbial colonization of the gastrointestinal tract and other mucosal surfaces might be initiated already *in utero*, continues at birth with the acquisition of microbes during vaginal delivery, and is completed during early postnatal life.<sup>6-9</sup>

It is now well established that allergic infants and children exhibit a reduced diversity of their gastrointestinal microbiota that is characterized by a predominance of Firmicutes

#### Abbreviations used

AF:	Alexa Fluor
APC:	Allophycocyanin
BATF3:	Basic leucine zipper ATF-like 3
BV:	Brilliant Violet
DC:	Dendritic cell
DT:	Diphtheria toxin
DTR:	Diphtheria toxin receptor
eGFP:	Enhanced green fluorescent protein
FACS:	Fluorescence-activated cell sorting
FITC:	Fluorescein isothiocyanate
FOXP3:	Forkhead box P3
GFP:	Green fluorescent protein
HDM:	House dust mite
HRP:	Horseradish peroxidase
IAV:	Influenza A virus
IRF4:	Interferon regulatory factor 4
LDA:	Linear discriminate analysis
MHCII:	MHC class II
MLN:	Mesenteric lymph node
NAL:	Nalidixic acid
OTU:	Operational taxonomic unit
OVA:	Ovalbumin
PAS:	Periodic acid–Schiff
PE:	Phycoerythrin
PerCP:	Peridinin-chlorophyll-protein complex
pfu:	Plaque-forming units
ROR $\gamma$ t:	Retinoic acid–related orphan receptor $\gamma$ t
T-bet:	T-box transcription factor
Treg:	Regulatory T
TSDR:	Regulatory T cell–specific demethylated region
VacA:	Vacuolating cytotoxin

and members of the Bacteroidaceae family.<sup>2</sup> In both developed and developing countries, the decreasing prevalence of immunomodulatory microbes, such as intestinal helminths<sup>10,11</sup> or *Helicobacter pylori*,<sup>12-15</sup> is significantly associated with an increased risk for allergic disease, especially in pediatric populations.

We have reported that neonatal infection of mice with *H pylori* protects effectively against the airway hyperresponsiveness, pulmonary inflammation, and goblet cell metaplasia that are hallmarks of experimental models of asthma induced by ovalbumin (OVA) or house dust mite (HDM) allergen sensitization and challenge.<sup>16-19</sup> The experimental infection of adult animals had no or much weaker effects on allergy parameters, a finding that is in agreement with epidemiologic data suggesting that older adults benefit less from harboring *H pylori* than children, adolescents, and young adults.<sup>12,13,20,21</sup> The underlying protective mechanism involves tolerogenic subsets of dendritic cells (DCs) that, in the context of an *H pylori* infection, drive the differentiation and suppressive activity of Treg cells.<sup>16,17,19,22</sup> Interestingly, the immunomodulatory activity of *H pylori* depends on 2 determinants, the vacuolating cytotoxin (VacA) and  $\gamma$ -glutamyl-transpeptidase (GGT), which are on the one hand required for the protective effects of the live infection and on the other hand recapitulate many of the benefits associated with live infection when administered in purified form.<sup>18,22,23</sup>

Here we hypothesized that the perinatal transmaternal exposure (ie, exclusively through the mother) to immunomodulatory

molecules of *H pylori* that occurs *in utero* or during lactation can recapitulate the benefits of *H pylori* infection early in life. To test this idea, we perinatally exposed animals to *H pylori* extract or purified VacA and evaluated their response to allergens in 2 models of allergen-induced airway inflammation. We further examined the immunologic, microbial metagenomic, and epigenetic correlates of perinatal exposure to *H pylori* to identify possible determinants and biomarkers of transmaternal immunomodulation. Finally, we used viral and bacterial infection models to address whether perinatal exposure to bacterial immunomodulators results in generalized immunosuppression.

## METHODS

### Study approval

All animal experimentation was reviewed and approved by the Zurich Cantonal Veterinary Office (licenses 170/2014 and 140/2017 to A.M. and 210/2014 to C.M.).

### Animal experimentation

C57BL/6 mice were purchased from Janvier (Le Genest—Saint-Isle, France), and forkhead box P3 (Foxp3)<sup>eGFP-DTR</sup> (B6.129[Cg]-Foxp3tm3<sup>IDTR/GFP</sup>Ayr/J, 016958), as well as OT-II (B6.Cg-Tg[TcrαTcrβ]425Cbn/J) mice, were purchased from the Jackson Laboratory (Bar Harbor, Me) and included in experiments at 5 to 8 weeks of age. For induction of acute HDM-induced airway inflammation, mice were briefly anesthetized and subsequently subjected to 6 intranasal injections of HDM extract (XPB70D3A25 *Dermatophagoides pteronyssinus*; Greer Laboratories, Lenoir, NC) on day 0 (1 μg) and on days 8 to 12 (10–15 μg depending on extract lot). Mice were killed on day 15. Transgenic Foxp3-enhanced green fluorescent protein (eGFP)-diphtheria toxin receptor (DTR) mice were intraperitoneally treated 4 times with 1 μg of diphtheria toxin (DT; D0564-1MG; Sigma, St Louis, Mo) during days 5 to 12 of the HDM protocol. The OVA-induced model of airway inflammation involved sensitization with 20 μg of OVA (A5503; Sigma) adjuvanted with Alum Injunct (77161; Thermo Scientific, Waltham, Mass) by means of intraperitoneal injection on days 0 and 14, followed by challenge on days 28, 29, and 30 with 1% aerosolized OVA in PBS by using an ultrasonic nebulizer.

At the study end point, blood was collected, and serum was prepared. Lungs were lavaged through the trachea with 1 mL of PBS. Bronchoalveolar lavage fluid cells were counted by using trypan blue dye exclusion. Differential cell counts of macrophages, lymphocytes, neutrophils, and eosinophils were performed on cytocentrifuged preparations stained with the Microscopy Hemacolor-Set (Merck, Whitehouse Station, NJ). One lung lobe was collected and homogenized, total protein was isolated, and the concentration was determined by using the BCA Protein Assay Kit (23227; Thermo Scientific). For histopathology, lungs were fixed by means of inflation and immersion in 10% (vol/vol) formalin and embedded in paraffin. Tissue sections were stained with hematoxylin and eosin and periodic acid–Schiff (PAS) and examined in blind fashion on a BX40 Olympus microscope (Olympus, Center Valley, Pa). Peribronchial inflammation was scored on a scale from 0 to 4. PAS-positive goblet cells were quantified per 1 mm of basement membrane, as described previously.<sup>16</sup> Scoring and goblet cell quantification were performed on 3 to 4 sections per mouse cut at different depths of 20-μm intervals and ideally on more than 1 lung lobe, although this was not always possible.

For production of *H pylori* extract, bacterial cultures of the *H pylori* strain PMSS1 were pelleted, washed with PBS, and subjected to 3 freeze-thaw cycles and homogenization by using a pressure cell homogenizer (Stansted SPCH-18). The same procedure was used to produce *Escherichia coli* (BL21, DE3) extract. The homogenate was centrifuged at 3000g, the resulting supernatant was filter sterilized, and the protein concentration was determined as above. To prevent microbial contamination during cultivation of *H pylori*, we generally used media supplemented with vancomycin and regularly checked for microbial contamination by streaking on selection plates containing antibiotics to which *H pylori* is naturally resistant. Oligomeric s1m1-type VacA was purified from culture supernatants of *H pylori*

strain 60190 expressing Strep-tagged VacA through a Strep-Tactin resin (IBA Lifesciences, Göttingen, Germany), as described previously.<sup>24</sup> The dose of extract and VacA was adjusted to the age of the mice and application mode: extract (oral), 50 μg for neonates and 200 μg for adult mice; VacA (intraperitoneal), 5 to 20 μg; and VacA (oral), 5 to 20 μg. Neonates were treated with VacA or extract 1 to 2 times per week. Dams were treated 2 to 3 times per week during the entire pregnancy and lactation phase. For microbiota transplantation, the cecal content of transmaternally treated or untreated adult mice was isolated and suspended in PBS, and the weight per milliliter of PBS was adjusted, centrifuged at 300g, and filtered through a cell strainer before gavage to 7-day-old pups.

### IL-13- and HDM-specific IgE ELISA

The concentration of IL-13 in lung homogenates was determined by using the Mouse IL-13 ELISA Kit (88-7137-88; eBioscience, San Diego, Calif). Quantification of serum HDM-specific IgE was performed by coating high-affinity 96-well plates with 100 μL of 25 μg/mL HDM extract in carbonate-bicarbonate coating buffer overnight at 4°C. After washing and blocking, diluted samples were incubated for 2 hours before washing again and addition of a horseradish peroxidase (HRP)-coupled IgE-specific antibody (GTX77227; GeneTex, Irvine, Calif) for detection. HRP substrate was added, and the absorbance was measured on a plate reader. Arbitrary units were calculated by using a standard curve determined by using serial dilution of a serum mix processed on the same plate.

### Cytometric bead assay

Thirteen different cytokines were analyzed by using the Mouse Th Cytokine Panel LEGENDplex assay (740005; BioLegend, San Diego, Calif).

### Treg cell-specific demethylated region methylation analysis

Total mesenteric lymph node (MLN) cells of male C57BL/6 mice were isolated by using collagenase type IV (C5138; Sigma) digestion and filtering through a cell strainer. Male mice had to be used because in female mice one X-chromosome is inactivated by means of DNA methylation, which biases the results obtained for the second active copy. After fixation, permeabilization, and washing, cells were stained with anti-mouse CD4-fluorescein isothiocyanate (FITC; 100510; BioLegend) and Foxp3-allophycocyanin (APC) antibodies (17-5773-82; eBioscience). CD4<sup>+</sup>Foxp3<sup>+</sup> and CD4<sup>+</sup>Foxp3<sup>-</sup> cells were sorted on a FACSAria. Genomic DNA was isolated from sorted cell subsets by using the NucleoSpin Tissue kit (Macherey-Nagel, Duren, Germany). An additional step was added to the manufacturer's protocol to remove formaldehyde-induced crosslinking. Briefly, Chelex-100 beads (Bio-Rad Laboratories, Hercules, Calif) were added after the lysis step and incubated at 95°C for 15 minutes in a shaker. Chelex-100 beads were spun down, and the supernatant was transferred to a fresh tube.

After addition of an adjusted amount of 100% ethanol, additional purification steps were performed according to the manufacturer's protocol. Genomic DNA was converted with bisulfite by using the EZ DNA Methylation Kit (Zymo Research, Irvine, Calif), according to the manufacturer's instructions. The regulatory T cell-specific demethylated region (TSDR) was amplified by means of PCR and analyzed by pyrosequencing on a PSQ96MA instrument (Qiagen, Hilden, Germany), as previously described<sup>25</sup>; primers for sequencing were (in the 5' to 3' direction) S1 (CCATAC AAAACCCAAATTC); S2 (ACCCAAATAAAAATAATATAAATACT) S3 (ATCTACCCACAAAATTT) and S4 (AACCAAATTTTCTACCATT), which cover CpG motifs 3 to 12 of the TSDR core region.

### Flow cytometric analysis and cell sorting for quantitative RT-PCR

Total MLN cells of C57BL/6 or Foxp3-eGFP-DTR mice were isolated by filtering through a cell strainer. Cells from perfused lungs were isolated by mincing the tissue, followed by digestion with collagenase type IA

(C9891-500MG; Sigma) and mechanical disruption with a syringe and pushing through a cell strainer.

To assess DC allergen uptake and processing capacity, mice were challenged intranasally with 50  $\mu$ L of DQ-OVA (800  $\mu$ g/mL; D12053; Thermo Fisher Scientific) and Alexa Fluor (AF) 647-OVA (800  $\mu$ g/mL; 034784; Thermo Fisher Scientific) approximately 15 hours before death. After washing, the cells were stained in various combinations with mouse-specific antibodies targeting CD4-peridinin-chlorophyll-protein complex (PerCP)/Cy5.5 or Brilliant Violet (BV) 785 (116012 or 100552; BioLegend), CD45-BV650 (103151; BioLegend), the fixable viability dye eFluor780 (65-0865-14; eBioscience), T-cell receptor  $\beta$  chain-phycoerythrin (PE)/Cy7 (109222; BioLegend), Siglec-F-PE or BB515 or BV421 (552126, 56514, and 562681; BD, Franklin Lakes, NJ), CD16/CD32 Fc Block (101302; BioLegend), CD11c BV605 (117333; BioLegend), CD11b PerCP/Cy5.5 (101228; BioLegend), CD103-PE (121406; BioLegend), I-A/I-E-AF700 (107622; BioLegend), F4/80-APC (123116; BioLegend), CD8 $\alpha$ -BV510 or PE/Cy7 (100752 or 100722; BioLegend), Neuropilin-1-BV421 (145209; BioLegend), CXCR3-BV510 (126527; BioLegend), and CD3-biotin (100244; BioLegend) in combination with streptavidin-BV711 (405241; BioLegend). After fixation, permeabilization, and washing, cells were stained with antibodies for Foxp3-BV421 (126419; BioLegend) or Foxp3-FITC (11-5773-82; eBioscience), retinoic acid-related orphan receptor  $\gamma$ T (ROR $\gamma$ T)-PE-eFluor 610 (61-6981; eBioscience), and interferon regulatory factor 4 (IRF4)-PerCP-eFluor 710 (46-9858-80; eBioscience). In some experiments cells were restimulated *in vitro* in Iscove modified Dulbecco M medium supplemented with GolgiStop (51-2092KZ; BD), Brefeldin A (00-4506-51; eBioscience), phorbol 12-myristate 13-acetate (P-8139; Sigma), and ionomycin (I0634-1M; Sigma) before fixation and permeabilization for intracellular cytokine staining with anti-mouse IL-17-APC (506916; BioLegend) and IFN- $\gamma$ -AF488 (505815; BioLegend). Samples were analyzed on an LSR II Fortessa instrument, followed by detailed analysis with FlowJo software (TreeStar, Ashland, Ore). For fluorescence-activated cell sorting (FACS) of Treg cells, MLN cells or lung cells from Foxp3<sup>eGFP-DTR</sup> mice were stained with the fixable viability dye eFluor780 (65-0865-14; eBioscience) and antibodies targeting CD4 BV711 (100550; BioLegend) and Siglec-F-BV421 (562681; BD) and sorted for live CD4<sup>+</sup> green fluorescent protein (GFP)<sup>+</sup> cells on a FACS Aria. RNA of sorted cells was isolated with the RNeasy Mini Kit (74106; Qiagen), converted into cDNA, and subjected to TaqMan Real-Time PCR assay by using the primers Mm03024075 (*Hprt*), Mm00475162 (*Foxp3*), Mm01178820 (*Tgfb1*), and Mm01288386 (*Ilio*; all from Thermo Fisher Scientific). Samples were run on a LightCycler 480 and normalized to the housekeeping gene *Hprt*.

## RNA sequencing

Lung Treg cells were sorted, as described above, in the section "Flow cytometric analysis and cell sorting for quantitative RT-PCR." RNA was isolated by using the RNeasy Micro Kit (Qiagen), and RNA quality was assessed by using the Bioanalyzer 2100. The TruSeq RNA Sample Prep Kit v4 (Illumina, San Diego, Calif) was used for library preparation, and sequencing was performed on the Illumina HiSeq 2500 instrument. RNA sequencing reads were quality checked with FastQC, which computes various quality metrics for the raw reads. RNA sequencing reads were mapped to the GRCm38 mouse reference genome by using STAR. Reads were counted according to Ensembl gene annotation by using the featureCounts function in the Rsubread Bioconductor package. The EdgeR package was used to conduct statistical analysis of differential expression. The Treg cell RNA sequencing data reported in this article are available in the Gene Expression Omnibus database (<http://www.ncbi.nlm.nih.gov/gds>) under accession number GSE116116.

## Influenza A infection

Seven-week-old mice were anesthetized by using intraperitoneal injection of 0.05 mg/kg fentanyl (Sintetica, Mendrisio, Switzerland), 5 mg/kg midazolam (Dormicum; Roche, Mannheim, Germany), 0.5 mg/kg medetomidin (Dorbene; Gräub) and infected intranasally with 200 plaque-forming units (pfu) of influenza A H1N1 strain A/Puerto Rico/8/1934 (PR8; Charles River, Wilmington, Mass) diluted in 30  $\mu$ L of PBS (Gibco, Grand Island, NY). Anesthesia was antagonized by means of

intraperitoneal injection of 2.5 mg/kg atipamezole (Alzane; Gräub), 1.2 mg/kg naloxone (Swissmedic, Bern, Switzerland), and 0.5 mg/kg flumazenil (Anexate; Roche).

Mice were killed by means of CO<sub>2</sub> asphyxiation on day 9 after infection. Blood was obtained by means of heart puncture. Lungs were perfused with cold PBS and extracted. Extracted lungs were cut into small pieces. After digestion with 2 mg/mL Collagenase A (C9891; Sigma) and 40  $\mu$ g/mL DNase A (7002221; Roche) for 45 minutes at 37°C, a single-cell suspension was obtained by passing the tissue through a cell strainer of 40  $\mu$ m. Leukocytes were isolated by using Percoll gradient centrifugation (GE Healthcare, Fairfield, Conn). Isolated leukocytes were restimulated *in vitro* in RPMI 1640 medium (Gibco) with 2  $\mu$ g/mL rat anti-mouse CD28 (553294; BD) and 10  $\mu$ g/mL PR8-specific epitopes Nucleoprotein<sub>1366-374</sub> and hemagglutinin<sub>211-225</sub> or irrelevant control peptide OVA<sub>257-264</sub> (peptides&elephants, Brandenburg, Germany). Brefeldin A (BD) was added after 1 hour of restimulation at 5  $\mu$ g/mL. After an additional incubation time of 4 hours, cells were stained with FITC-labeled rat anti-mouse CD8 (clone 53-6.7; eBioscience), fixed, and permeabilized, according to the manufacturer's instructions (Cytofix/Cytoperm kit, 554714; BD) and intracellularly stained with PE-labeled rat anti-mouse IFN- $\gamma$  (554412; BD). Cells were subjected to flow cytometric analysis with the FACSCanto II (BD). For determination of PR8-specific IgG titers, adsorbent 96-well ELISA plates (NUNC) were coated with PR8 virus at  $5 \times 10^5$  pfu/mL overnight at 4°C. Virus was inactivated by means of UV irradiation of  $2 \times 240$  mJ. Blood was collected in Microtainer tubes (365967; BD) and spun at 3500 rpm for 10 minutes to obtain serum. Serial dilutions of serum in PBS were distributed in ELISA plates. Bound IgG was detected with HRP-coupled goat anti-mouse IgG (Jackson Laboratories) and visualized by means of incubation with substrate (TMB; Sigma). The reaction was stopped with H<sub>2</sub>SO<sub>4</sub> 1N solution, and plates were acquired on a Tecan infinite M200 Pro Reader (Tecan), at 450 nm and 620 nm. Values at 620 nm were subtracted from readings at 450 nm.

## Citrobacter rodentium infection

The nalidixic acid (NAL)-resistant *C rodentium* strain ICC169 was grown overnight at 37°C in Luria broth supplemented with NAL (50  $\mu$ g/mL; Sigma). Mice were infected orally with  $5 \times 10^8$  bacteria for 12 days. To assess *C rodentium* colonization, cecal and colonic tissues were homogenized in PBS, diluted, and plated on Luria broth plates supplemented with NAL. Colonies were counted after 18 hours of culture at 37°C. Colonic and cecal bacterial loads were normalized to tissue weight. Colonic lamina propria preparations were stained and flow cytometrically analyzed, as described under "Flow cytometric analysis."

## In vitro coculture of naive T cells and CD11c<sup>+</sup> antigen-presenting cells

Total spleen cells from OT-II mice were filtered through a 40- $\mu$ m cell strainer. After red blood cell lysis with ACK buffer, the remaining cells were stained with antibodies targeting CD4 BV711 (100549; BioLegend), CD25-FITC (102005; BioLegend), CD44-AF647 (103017; BioLegend), CD62L-PE (104407; BioLegend), T-cell receptor  $\beta$ -PE-Cy7 (109222; BioLegend), CD11c-V450 (560369; BD), MHC class II (MHCII)-AF700 (107622; BioLegend) and the viability dye eFluor780 (65-0865-14; eBioscience). Naive T cells and CD11c<sup>+</sup>MHCII<sup>+</sup> antigen-presenting cells were FACS sorted on a FACS Aria and subsequently cocultured at a ratio of 5:1 in the presence of 1  $\mu$ g/mL OVA peptide 323-339 (EMC BAP-250) and 5 ng/mL recombinant murine TGF- $\beta$ 1 (7666-MB; R&D Systems, Minneapolis, Minn) for 72 hours. Staining of Treg cells and FACS analysis was conducted, as described in "Flow cytometric analysis."

## Library preparation for microbiome analyses

Gastric tissue and ileal, cecal, and colonic tissue and their contents were collected after necropsy and immediately frozen in liquid nitrogen and stored at -80°C until DNA extraction. DNA was extracted with the DNeasy PowerSoil HTP 96 Kit (Qiagen), and the V4 region of the bacterial 16S

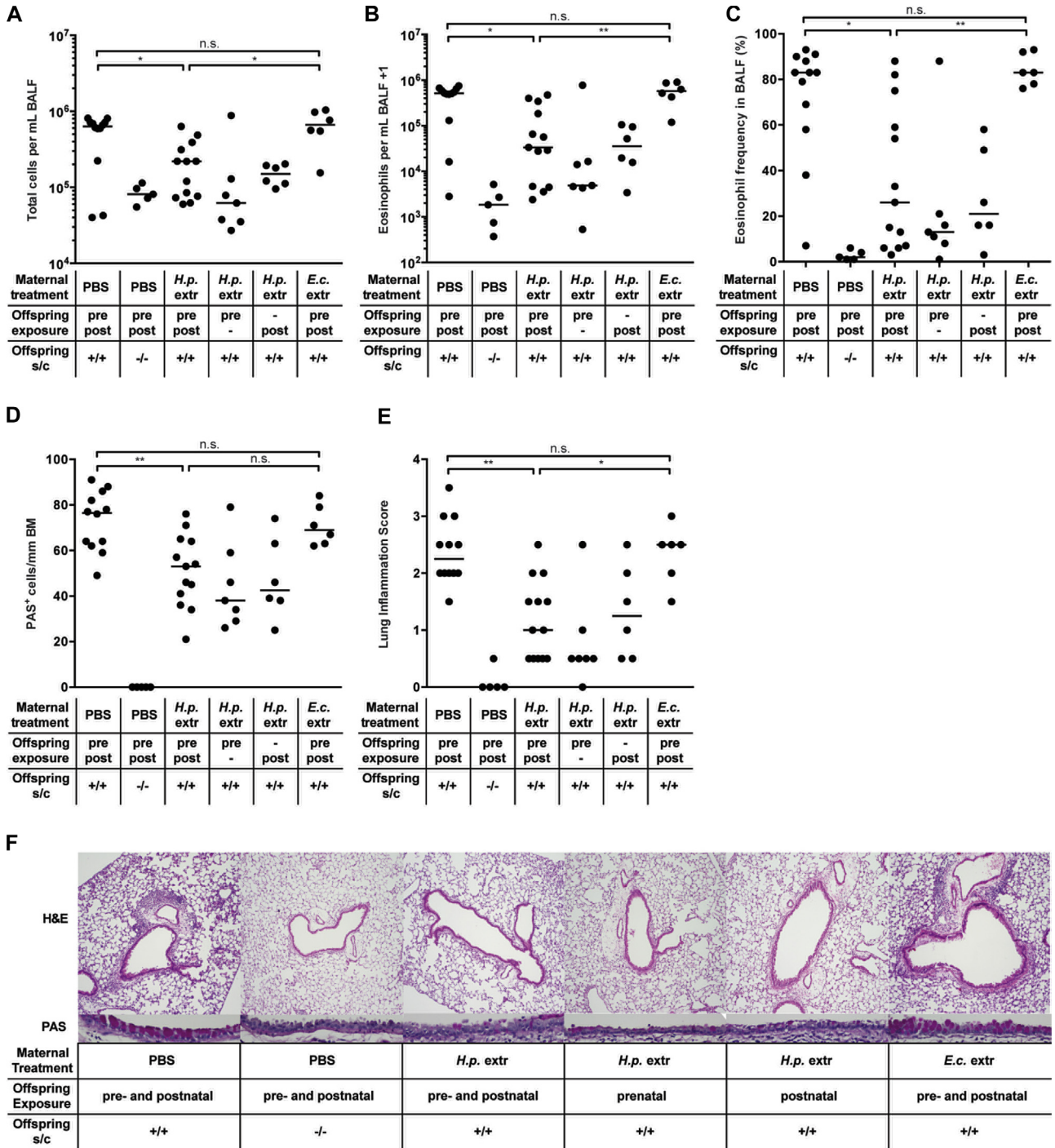


**FIG 1.** Perinatal transmaternal exposure to *H. pylori* but not *E. coli* extract protects against HDM-induced allergic airway inflammation. Mice were either prenatally (*pre*) or postnatally (*post/prepost*) transmaternally exposed to *H. pylori* extract (*H.p. extr*), *E. coli* extract (*E.c. extr*) or PBS treatment through 2 to 3 weekly oral gavages of the dams during pregnancy, lactation, or both. Litter swaps were conducted at birth where necessary to avoid unwanted exposures. At 6 weeks of age, offspring were sensitized and challenged (*s/c*) intranasally with HDM allergen. Negative controls were sensitized and challenged with PBS only. **A**, Total leukocytes in 1 mL of bronchoalveolar lavage fluid (BALF). **B**, Total eosinophils in 1 mL of BALF. **C**, Eosinophil frequencies in BALF. **D-F**, Pulmonary inflammation and goblet cell metaplasia, as assessed on stained lung sections. *BM*, basement membrane; *H&E*, hematoxylin and eosin. Representative sections are shown in Fig 1, *F*. In Fig 1, *A-E*, each symbol represents 1 mouse. Results were pooled from 2 independent experiments. *Horizontal lines* indicate medians; ANOVA with Dunn multiple comparison correction was used for calculation of *P*-values. \**P* < .05 and \*\**P* < .01. *n.s.*, Not significant.

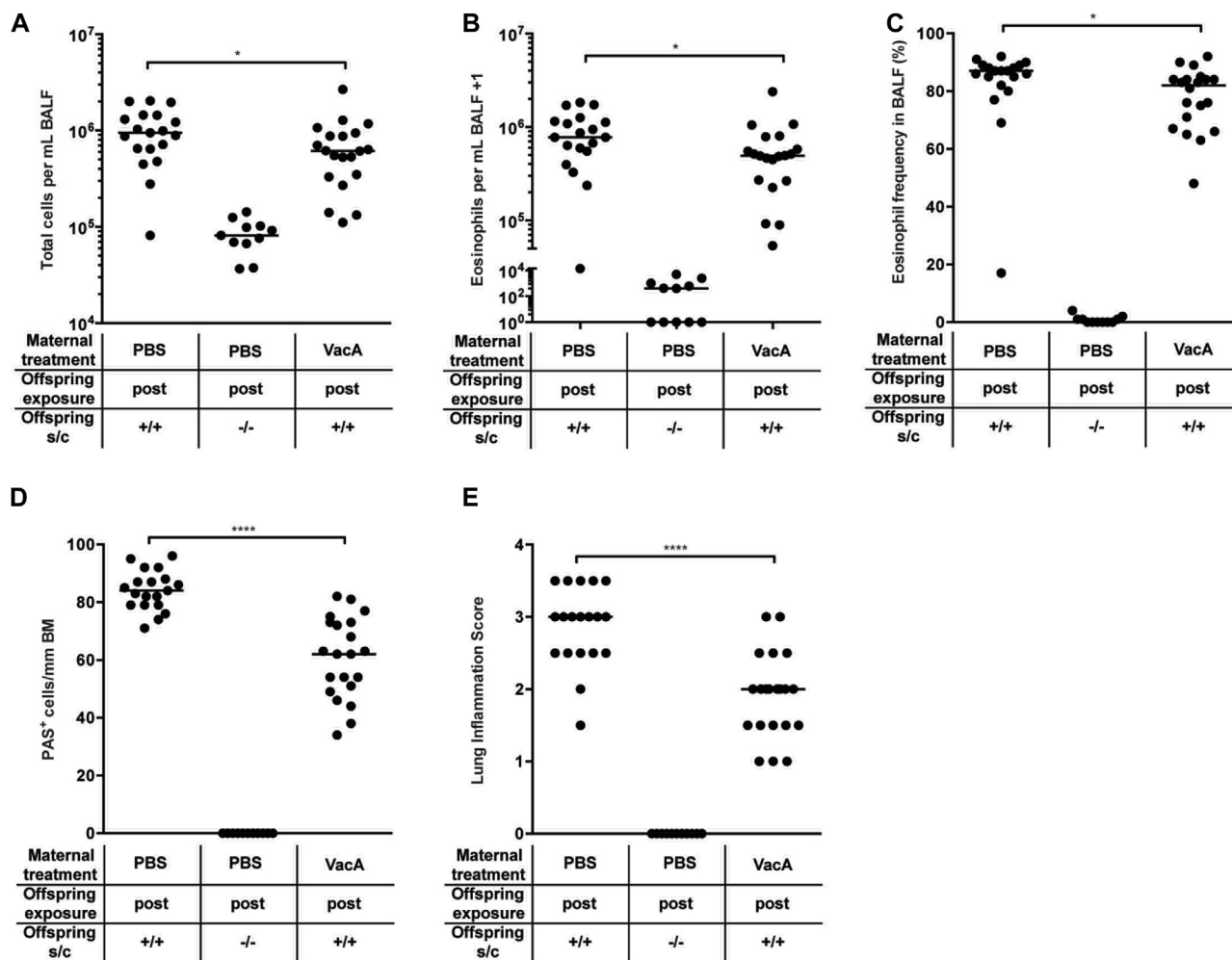


**FIG 2.** Postnatal transmaternal exposure to *H pylori* VacA protects against HDM-induced allergic airway inflammation. Mice were transmaternally exposed postnatally (*post*) to *H pylori* VacA through twice-weekly intraperitoneal treatments of the dams with 20  $\mu$ g of purified VacA during lactation. Offspring of PBS-treated dams were used as controls. At 6 weeks of age, offspring were sensitized and challenged (*s/c*) intranasally with HDM allergen. Negative controls were sensitized and challenged with PBS only. **A**, Total leukocytes in 1 mL of bronchoalveolar lavage fluid (BALF). **B**, Total eosinophils in 1 mL of BALF. **C**, Eosinophil frequencies in BALF. **D** and **E**, Pulmonary inflammation and goblet cell metaplasia, as assessed on stained lung sections. *BM*, basement membrane. In Fig 2, *A-E*, each symbol represents 1 mouse. Results were pooled from 3 independent experiments. Horizontal lines indicate medians; an unpaired Mann-Whitney *U* test was used for statistical analyses. \**P* < .05 and \*\*\*\**P* < .0001.

rRNA gene was amplified in triplicate by using barcoded fusion primers (F515/R806).<sup>26</sup> Amplicon replicates were pooled, and the DNA was quantified with Quant-iT PicoGreen (Invitrogen, Carlsbad, Calif). A maximum of 94 samples were then pooled at a concentration of 20 nmol/L, purified with a QIAquick PCR purification kit (Qiagen), and quantified with a Qubit 2.0 Fluorometer (Life Technologies, Grand Island, NY). Finally, these samples were pooled at equal molar concentrations and sequenced on the Illumina MiSeq platform.

### Microbiome analysis

By using QIIME 1.9.1, forward and reverse paired-end reads were trimmed and joined before being demultiplexed, filtered, and analyzed. Open-reference operational taxonomic unit (OTU) picking was performed by using the Greengenes Database Consortium (May 2017). Unweighted UniFrac distances were calculated, and 2-dimensional principal coordinate plots were generated in QIIME. Statistical significance was determined by using the Adonis or Anosim tests. A linear discriminate analysis (LDA) effect size was performed to determine OTUs that were significantly altered by treatment. Taxa were classified as significantly different between groups when the log<sub>10</sub>

LDA score was greater than 2.0 and the *P* value was less than .05, as determined by using ANOVA. Taxa were summarized at the genus level, and unclassified taxa were removed.

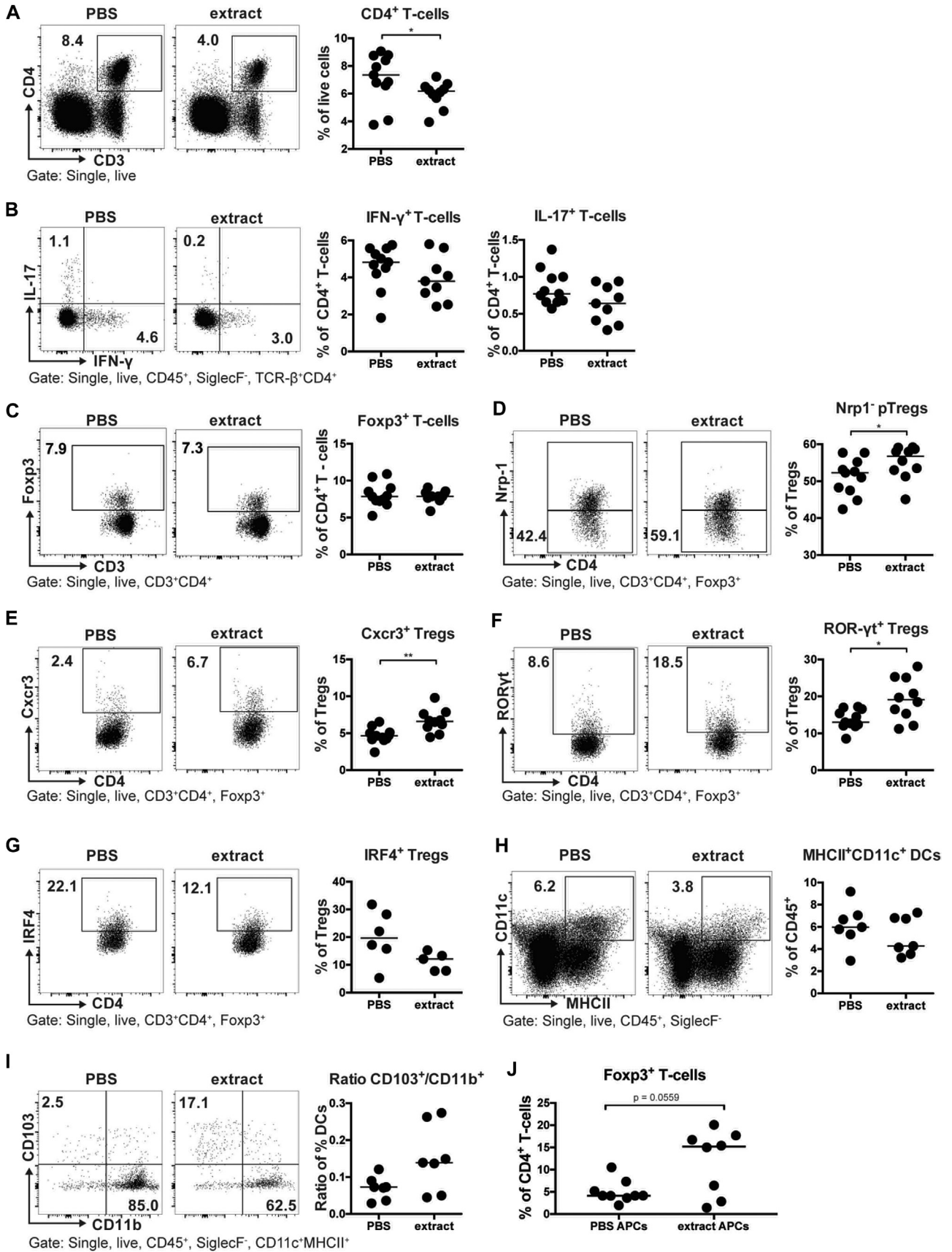
### Statistical analysis

GraphPad Prism 6 software (GraphPad Software, La Jolla, Calif) was used for all statistical analyses. Unless specified otherwise, symbols in graphs represent individual mice, and horizontal lines indicate medians. The Mann-Whitney test or ANOVA with the Dunn correction for multiple comparisons was used to assess for significant differences.

## RESULTS

### Perinatal exposure to *H pylori* extract reduces symptoms of HDM-induced allergic airway inflammation

To address whether administration of *H pylori* extract to pregnant or lactating mice reduces allergy symptoms of their



offspring on allergen exposure later in life, we intragastrically treated female mice with twice-weekly doses of *H pylori* extract generated using nondenaturing pressure homogenization. *H pylori* extract was orally administered either during the 3 weeks of pregnancy, during lactation, or both, with the first 2 treatments requiring litter swapping at birth (see schematic in Fig E1, A, in this article's Online Repository at [www.jacionline.org](http://www.jacionline.org)). All offspring received an intranasal dose of HDM allergen for the purpose of allergic sensitization once they had reached 6 weeks of age, followed by intranasal HDM challenge on days 8 to 12 after sensitization (see Fig E1, B).

Both prenatal and postnatal exposure of the offspring (ie, *in utero* or during lactation), as well as the combined treatment, efficiently reduced all assessed parameters of airway inflammation, with strongly diminished overall leukocyte infiltration of the bronchoalveolar lavage fluid, strongly reduced eosinophilia, lower inflammation scores, and fewer PAS-positive goblet cells counted in the airway epithelium (Fig 1, A-F). HDM-specific serum IgE titers and pulmonary expression of the T<sub>H</sub>2 cytokines IL-5 and IL-13 were reduced as well (see Fig E1, C-E); additional cytokines (IFN- $\gamma$ , TNF- $\alpha$ , IL-2, IL-4, IL-6, IL-10, IL-17A, IL-21, and IL-22) were quantified by means of cytometric bead array of lung extracts but did not change on HDM sensitization and challenge (data not shown). The parallel administration of *E coli* extract had no measurable effect on the various parameters of allergen-induced airway inflammation, suggesting that the observed protection is specific to *H pylori* (Fig 1, A-F, and see Fig E1, C-E). Interestingly, we found the protective effects of extract exposure *in utero* or during lactation to be quite comparable in magnitude to the direct intraperitoneal or intragastric treatment of newborn pups with extract (see Fig E1, F-J) and to not be biased by litter sizes or sex (data not shown).

To address whether perinatal extract treatment induces general immunosuppression and thereby increases the susceptibility of the offspring to pulmonary challenge with influenza A virus (IAV),<sup>27</sup> we infected perinatally (prenatally and postnatally) treated offspring with 200 pfu (0.4 HAU) of IAV. The infection triggered clearly detectable weight loss, as well as high titers of PR8-specific IgG, with high titers correlating well with more pronounced weight loss (see Fig E1, K-M). The restimulation of lung leukocyte preparations with the influenza antigens NP1 and HA revealed strong influenza-specific CD8<sup>+</sup> T-cell responses (see Fig E1, N). Perinatal *H pylori* extract treatment did not measurably affect the magnitude of the IAV-specific readouts (see Fig E1, K-N), suggesting that the reduced severity of allergic airway inflammation is not likely to be due to general immunosuppression. This conclusion was further supported by

an acute bacterial infection model using *C rodentium*; transmaternally extract-treated animals were as effective at generating *C rodentium*-specific T<sub>H</sub>1 and T<sub>H</sub>17 responses and at controlling the infection as PBS-treated animals (see Fig E1, O-Q).

### Postnatal exposure to the *H pylori* immunomodulator VacA reduces HDM-induced allergic airway inflammation

We have previously attributed the allergy-protective effects of *H pylori* to its secreted immunomodulator VacA, which is both necessary and sufficient for conferring protection against OVA- and HDM-induced allergic airway inflammation on the one hand and food allergy driven by OVA or peanut allergen exposure on the other.<sup>18,22,28</sup> Because intraperitoneal injection was not feasible in pregnant dams, we administered VacA purified from culture supernatants of *H pylori* either intraperitoneally during lactation or orally during pregnancy and lactation. Both treatments, administered twice weekly reduced the bronchoalveolar infiltration and eosinophilia, as well as lung inflammation and goblet cell metaplasia, associated with HDM-induced allergic airway inflammation (Fig 2 and see Fig E2, A-E, in this article's Online Repository at [www.jacionline.org](http://www.jacionline.org)). However, we found transmaternally administered VacA to be less beneficial in terms of reducing allergy severity than the direct intraperitoneal treatment of newborn offspring with VacA (see Fig E1, F-J). The combined results suggest that the *H pylori* immunomodulator VacA suppresses hallmarks of allergic airway inflammation not only when present in the context of a live infection but also when administered in purified form to pregnant or lactating dams or to pups during the first weeks of life.

To address whether exposure of the offspring to (however minuscule) amounts of extract *in utero* or during lactation was required for the protective effects or tolerizing treatment of the mother from her own neonatal period onward and was sufficient to confer protection, we initiated the treatment of prospective mothers at 6 days of age but discontinued it before mating. The unexposed offspring of such tolerized mothers did not show evidence of protection against HDM-induced airway inflammation (see Fig E2, F-J), indicating that exposure to extract through the placenta or milk is a prerequisite for protection.

To rule out that transmaternal exposure to *H pylori* extract protects against HDM but not other allergens, we examined possible protective effects in the OVA model of allergic airway inflammation. Interestingly, the protective effects of transmaternal exposure to *H pylori* were just as strong in this model as in

**FIG 3.** Perinatal transmaternal exposure to *H pylori* extract skews lung T-cell responses toward specific Treg cell subsets. **A-I**, Mice were transmaternally prenatally and postnatally exposed to *H pylori* extract or PBS during pregnancy and lactation. At 6 weeks of age, lung leukocytes were analyzed by using multicolor flow cytometry. Fig 3, A, CD4<sup>+</sup> T-cell frequencies among all leukocytes; representative FACS plots are shown on the left. Fig 3, B, T<sub>H</sub>1 and T<sub>H</sub>17 cell frequencies among all CD4<sup>+</sup> T cells of the mice shown in Fig 3, A. Fig 3, C, Foxp3<sup>+</sup> Treg cell frequencies of the same mice. Fig 3, D, Peripherally induced Treg (*pTreg*) cell (Nrp-1<sup>-</sup>) frequencies among all Foxp3<sup>+</sup> Treg cells. Fig 3, E-G, Frequencies of Cxcr3<sup>+</sup>, ROR $\gamma$ t<sup>+</sup>, and IRF4<sup>+</sup> Treg cells among all CD4<sup>+</sup>FoxP3<sup>+</sup> Treg cells. Fig 3, H, MHCII<sup>+</sup>CD11c<sup>+</sup> DC frequencies among all pulmonary leukocytes. Fig 3, I, Ratios of CD103<sup>+</sup>CD11b<sup>-</sup> over CD103<sup>-</sup>CD11b<sup>+</sup> DCs of all mice shown in Fig 3, H; representative FACS plots are shown on the left. **J**, Frequencies of Foxp3<sup>+</sup> T cells among all CD4<sup>+</sup> OT-II T cells after 3 days of coculture with FACS-sorted splenic MHCII<sup>+</sup>CD11c<sup>+</sup> DCs. Data are pooled from 2 studies (Fig 3, A-F) or show the results of a representative experiment of at least 2 (Fig 3, G-J). Horizontal lines indicate medians; an unpaired Mann-Whitney *U* test was used throughout. \**P* < .05 and \*\**P* < .01.



the HDM model (see Fig E2, K and L), indicating that this form of allergy protection is independent of the allergen used.

### Perinatal exposure to *H pylori* extract skews lung T-cell responses toward Treg cells

We next performed a detailed analysis of the steady-state (unchallenged) lung T-cell and myeloid compartments using multicolor flow cytometry to identify immune correlates of the differential propensity of extract-treated and control mice to respond to HDM allergen. Mice that had been exposed perinatally (ie, *in utero* and until weaning) to *H pylori* extract exhibited generally lower pulmonary CD4<sup>+</sup> T-cell frequencies and lower T<sub>H</sub>1 and T<sub>H</sub>17 frequencies, as assessed by using intracellular cytokine staining for the signature cytokines IFN- $\gamma$  and IL-17, of *ex vivo*-restimulated leukocyte preparations than did the PBS-exposed offspring (Fig 3, A and B). Although the overall Foxp3<sup>+</sup> Treg cell frequencies did not differ among the 2 treatment groups, extract-exposed mice exhibited significantly greater frequencies of pulmonary neuropilin-negative Treg cells (which are enriched for peripherally induced Treg cells; see gating strategy in Fig E3, A, in this article's Online Repository at [www.jacionline.org](http://www.jacionline.org)) and of 2 Treg cell subsets that are associated with particularly high suppressive activity (ie, CXCR3<sup>+</sup> and ROR $\gamma$ t<sup>+</sup> Treg cells; Fig 3, C-F).<sup>29-32</sup> In contrast, the very abundant IRF4<sup>+</sup> Treg cell subset was not significantly different and, if anything, underrepresented in the lungs of extract-exposed mice (Fig 3, G). The shifts in T-cell populations appeared to be specific to the lung and were not observed in the MLNs (see Fig E3, B-H).

We next investigated whether DC subsets were quantitatively or functionally different in the lungs of extract- and PBS-exposed mice. DCs are critically required for the development of peripheral tolerance to antigens and allergens, and we have reported previously that the CD103<sup>+</sup> subset of DCs is overrepresented in the lungs of mice that are protected against allergic airway inflammation because of live infection with *H pylori*.<sup>22</sup> Although the overall frequencies of MHCII<sup>+</sup>CD11c<sup>+</sup> pulmonary DCs were somewhat lower in extract-treated relative to control animals (Fig 3, H), the ratio of CD103<sup>+</sup> to CD11b<sup>+</sup> DCs, which represent the 2 major resident DC populations, was greater (Fig 3, I). CD103<sup>+</sup>CD11b<sup>+</sup> DCs represent a minor (if any) population in the lung and do not change measurably on extract exposure (see Fig E3, I). As observed for T cells, DC populations in the MLNs did not differ depending on the perinatal exposure (see Fig E3, J-M).

To assess the functionality of DCs in the lung, we administered recombinant OVA protein that is coupled either to a constitutive fluorophore (AF647) or to a fluorophore that requires OVA processing and presentation in the context of MHCII molecules (DQ-OVA). Perinatal extract exposure did not measurably impair the ability of MHCII<sup>+</sup>CD11c<sup>+</sup> pulmonary DCs to sample or

process OVA (see Fig E3, N and O); however, the OVA-positive or DQ-OVA-positive DC populations recapitulated the general trend toward overrepresentation of CD103<sup>+</sup> DCs (see Fig E3, Q-S). Overall, our immunologic profiling efforts reveal the skewing of T-cell responses toward specific Treg cell subsets in extract-treated animals, which is consistent with the observed shifts favoring tolerogenic over immunogenic DC populations.

To examine possible direct systemic effects of transmaternal extract exposure on DCs, we sorted splenic CD11c<sup>+</sup>MHCII<sup>+</sup> DCs from 6-week-old, transmaternal extract-exposed or control offspring and cocultured them with naive splenic OT-II T cells in the presence of OVA peptide and recombinant TGF- $\beta$ . DCs from extract-exposed offspring showed a greater propensity to induce Foxp3 expression in naive T cells than their counterparts from control offspring (Fig 3, J), indicating their more pronounced tolerogenic activity in this setting.

### Perinatal exposure to *H pylori* extract or VacA affects the diversity and composition of gastrointestinal bacterial community structures

To address whether the perinatal exposure to *H pylori* extract or VacA not only has consequences for allergy severity and immunologic correlates of protection but also can affect the gastrointestinal microbiota, we performed 16S rRNA sequencing of 194 samples from the stomachs, ileums, ceca, and colons of 50 mice that were subjected to perinatal extract, VacA, or PBS treatment (ie, their mothers underwent oral gavage with extract, PBS, or VacA throughout pregnancy and lactation). We obtained an average of 6407 reads per sample. The sequencing depth was comparable across organs; to include 190 (ie, 98% of) samples, we rarified to 2000 reads, but results were similar with greater read depth and fewer samples (data not shown). In total, we identified 512 observed OTUs.

Examination of  $\beta$ -diversity using unweighted UniFrac analysis revealed a clear segregation of samples driven by anatomic site, as well as by treatment modality (see Fig E4, A and B, in this article's Online Repository at [www.jacionline.org](http://www.jacionline.org)). For each organ studied, samples clustered significantly by treatment group; this was most pronounced in the stomach and ileum (Fig 4, A and C). LDA effect size confirmed significant differences in relative abundances related to treatment. The largest differences were observed in the stomach and ileum; both VacA and extract treatment favored depletion of Firmicutes and Bacteroidetes in the stomach, whereas several taxa were strongly overrepresented at the class and order level (Fig 4, B and D). In the stomach VacA treatment resulted in depletion of *Allobaculum* species and enrichment of Ruminococcaceae *Clostridium* species (Fig 4, B). VacA treatment was associated with depletion of the taxa Clostridiaceae Candidatus Arthromitus (segmented filamentous bacteria), and treatment with either extract or VacA resulted in

**FIG 4.** Perinatal transmaternal exposure to *H pylori* extract induces shifts in the gastric and ileal microbiota. **A-D.** Mice were transmaternally prenatally and postnatally exposed to *H pylori* extract, VacA, or PBS through twice-weekly oral treatment of the dams during pregnancy and lactation. Gastric and ileal tissue was collected at necropsy and subjected to DNA extraction. The V4 region of the bacterial 16S rRNA gene was amplified and sequenced on the Illumina MiSeq platform. Fig 4, A and C, Unweighted UniFrac distances in a principal coordinate (PC) analysis plot, where samples were rarified at 2000 reads for the stomach (Fig 4, A) and ileal (Fig 4, C) tissue. The Adonis test was used to compare community structures between all treatment groups at both sites. Fig 4, B and D, OTUs that were significantly depleted or enriched as a consequence of the indicated treatments for the stomach (Fig 4, B) and ileum (Fig 4, D). LDA scores were generated with LefSE.

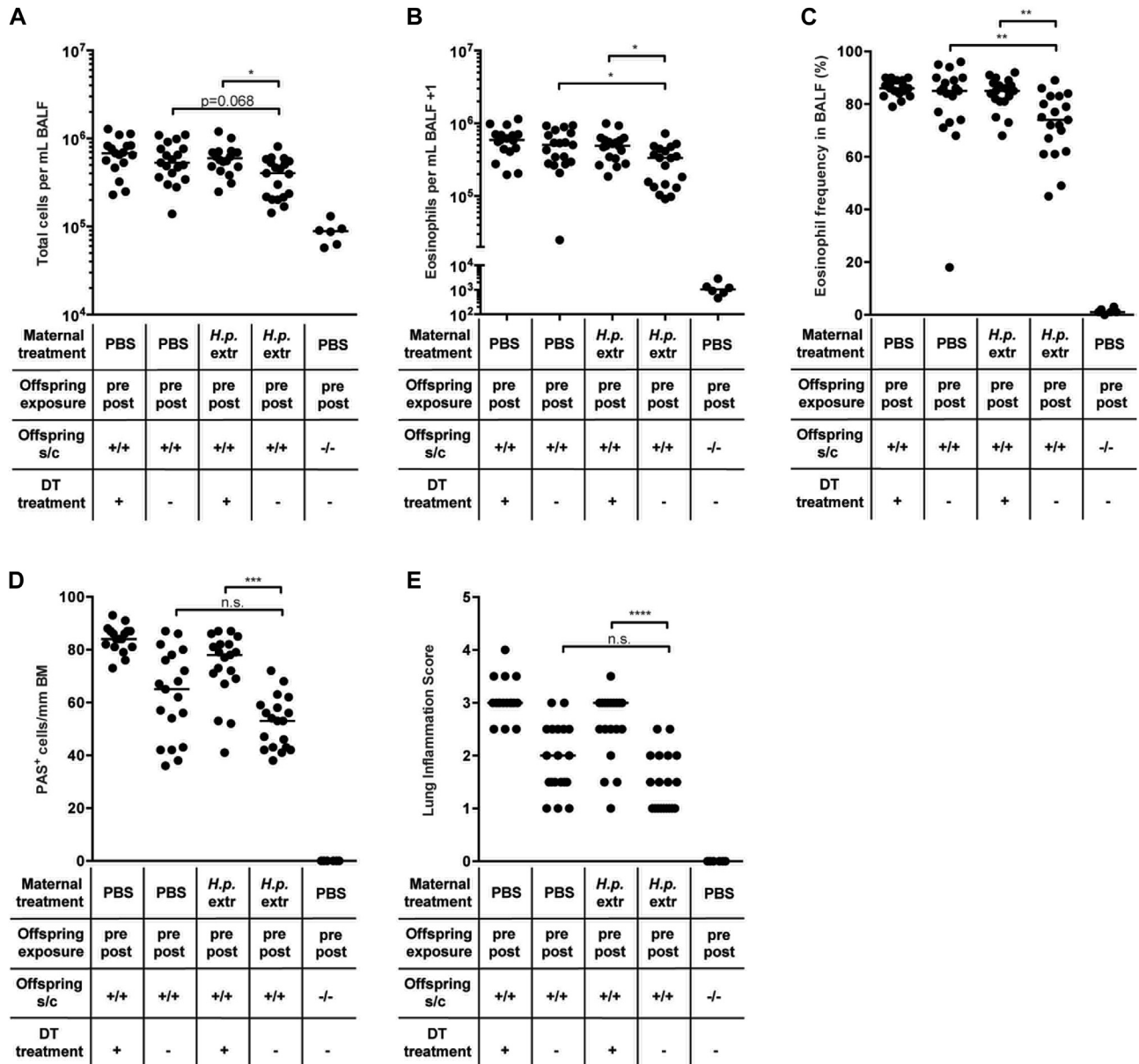


**FIG 5.** Depletion of Treg cells during HDM challenge abrogates allergy protection induced by means of perinatal transmaternal exposure to *H. pylori* extract. Foxp3<sup>DTR</sup> mice were transmaternally prenatally and postnatally exposed to *H. pylori* extract (*H.p. extr.*) or PBS. At 6 weeks of age, offspring were sensitized and challenged (*s/c*) intranasally with HDM allergen. Where indicated, mice received a total of 4 doses (spread across 8 days) of 1  $\mu$ g of DT just before and during HDM challenge. **A**, Total leukocytes in 1 mL of bronchoalveolar lavage fluid (BALF). **B**, Total eosinophils in 1 mL of BALF. **C**, Eosinophil frequencies in BALF. **D** and **E**, Pulmonary inflammation and goblet cell metaplasia, as assessed on stained lung sections. BM, Basement membrane. Each symbol represents 1 mouse. Results were pooled from 3 independent experiments. Horizontal lines indicate medians; ANOVA with Dunn multiple comparison correction was used for calculation of *P* values. \**P* < .05, \*\**P* < .01, \*\*\**P* < .001, and \*\*\*\**P* < .0001. *n.s.*, Not significant.

depletion of *Akkermansia* and *Desulfovibrio* species in the ileum (Fig 4, D). Thus the results from our metagenomics analysis suggest that perinatal exposure to *H. pylori* immunomodulators has clearly discernible effects on bacterial communities in the gastrointestinal tract much later in life, which might either be a cause or consequence of the skewing of steady-state immune parameters toward regulatory branches of the immune system.

To assess possible causality, we transplanted the cecal content of perinatally extract-exposed adult animals into neonates and subjected these animals to HDM sensitization and challenge as adults. Cecal transplantation was not sufficient to confer protection against allergic airway inflammation (see Fig E4, C-G), suggesting that changes in the gastrointestinal tract microbiota are probably a consequence rather than the cause of the immunomodulation that manifests in reduced allergy symptoms.

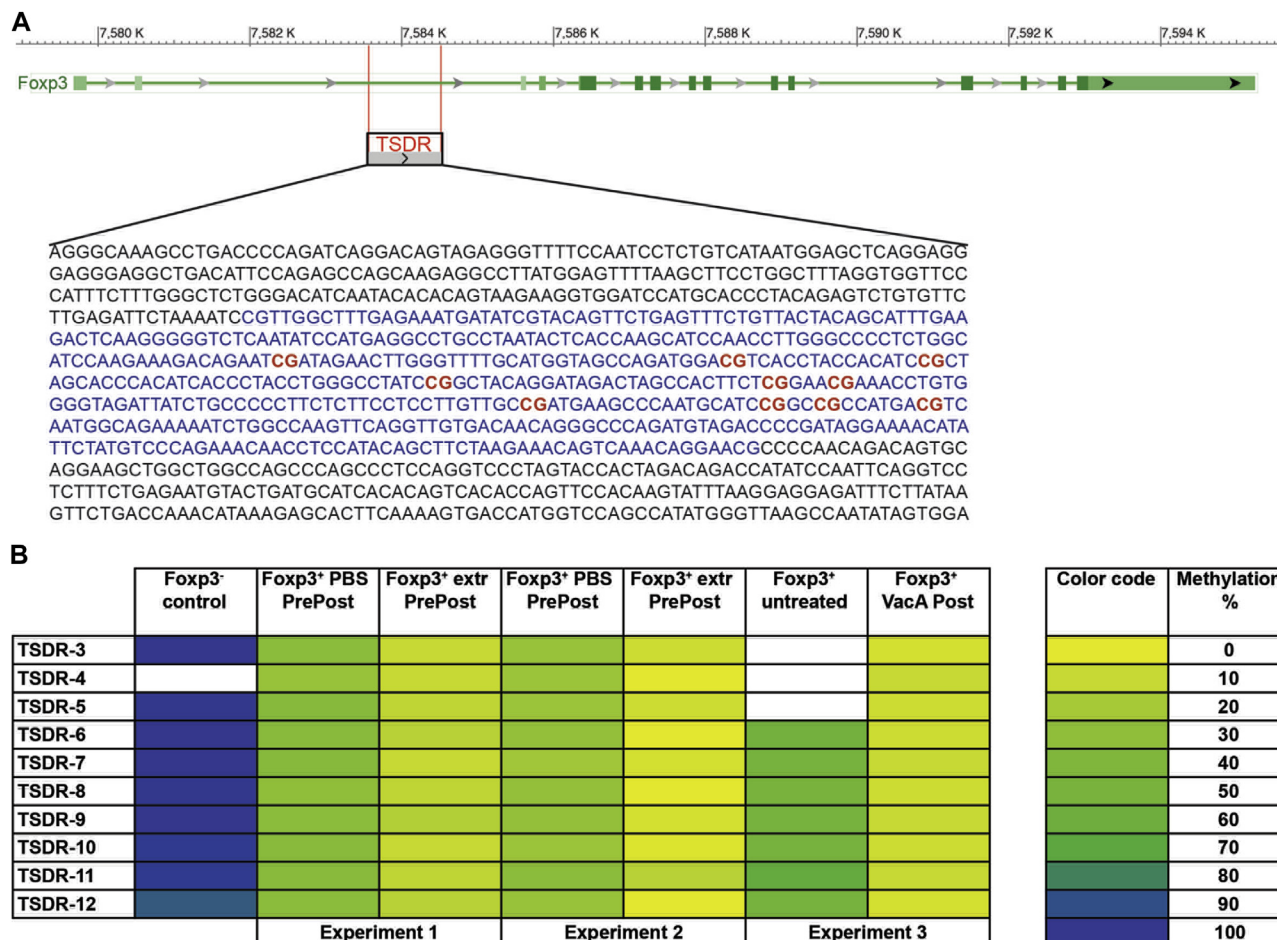


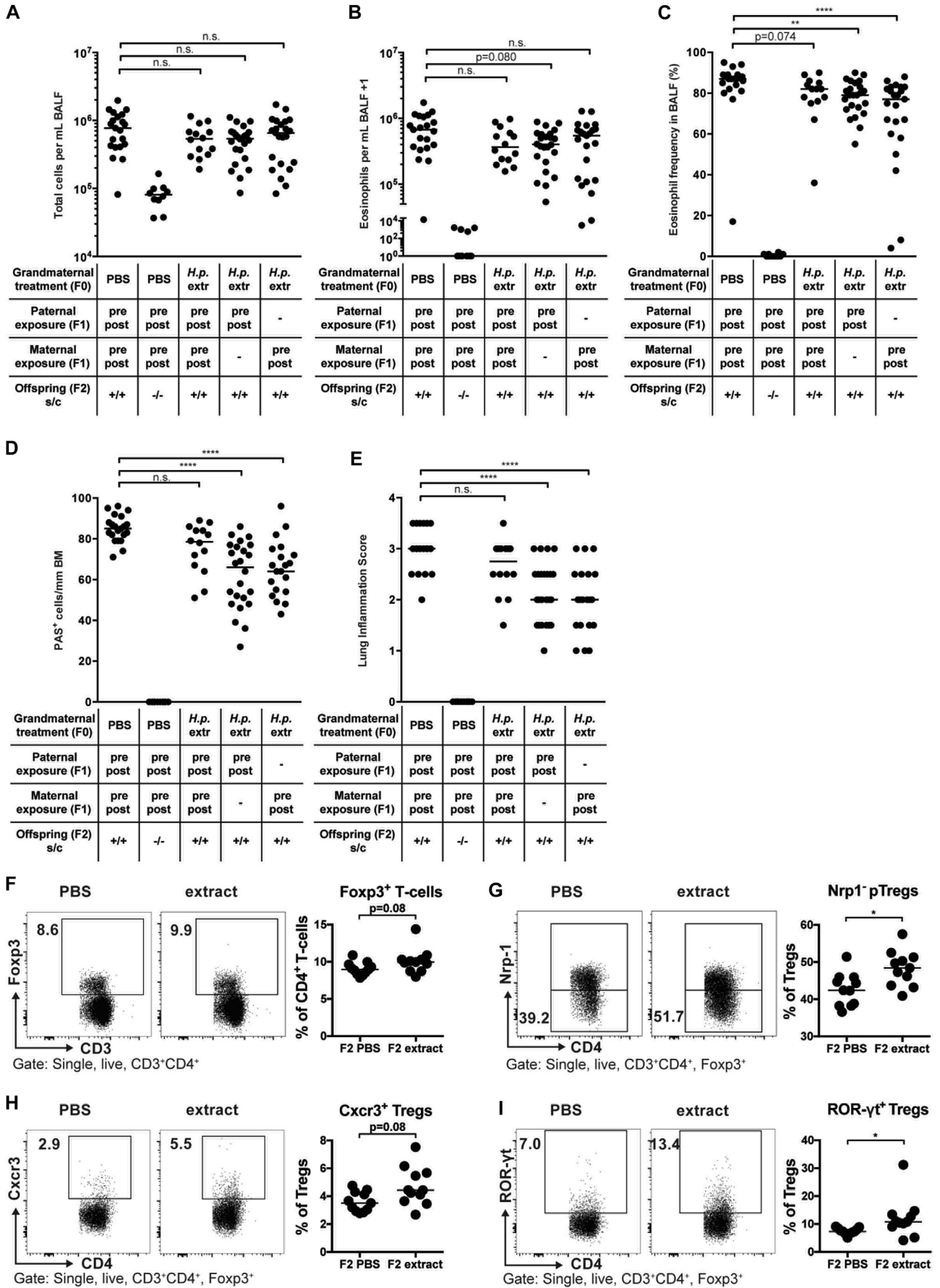
**FIG 6.** Perinatal transmaternal exposure to *H pylori* extract or VacA enriches for Treg cells with a demethylated *FOXP3* TSDR. Mice were transmaternally prenatally and postnatally exposed to *H pylori* extract or PBS or postnatally only to VacA through twice-weekly oral treatment of the dams during pregnancy and lactation (oral treatment with extract and PBS and intraperitoneal treatment with VacA). Foxp3<sup>+</sup> Treg cells and Foxp3<sup>+</sup> CD4<sup>+</sup> T cells were FACS sorted from the MLNs and subjected to DNA extraction. DNA was bisulfite converted and subjected to TSDR-specific pyrosequencing. **A**, Schematic representation of the *FOXP3* locus with the TSDR upstream of the TSS (retrieved by using BLAST). The CG-rich region is marked in blue, and CG motifs covered by pyrosequencing are labeled in red. **B**, Color-coded (right panel) methylation pattern of 10 CG dinucleotides within the TSDR region. White cells indicate sequences that did not yield interpretable results because of technical problems. Data are from 3 independent experiments (labeled experiments 1-3, with experiments 1 and 2 testing the effects of extract and experiment 3 testing the effects of VacA); cells from 5 to 10 male mice were pooled per treatment group before DNA extraction.

### Systemic depletion of Treg cells reduces the protective effects of *H pylori* extract on HDM-induced allergic airway inflammation

Having observed that in the steady-state perinatally extract-treated mice exhibit significantly higher frequencies of pulmonary Treg cell subsets with known or presumed suppressive activity than mock-treated control mice, we next set out to deplete Treg cells systemically during the challenge phase of our protocol of allergic airway inflammation.

To this end, HDM-sensitized mice expressing GFP and the DTR under the control of the *Foxp3* locus (Foxp3<sup>DTR</sup>)<sup>33</sup> received a total of 4 doses of DT a few days before and during allergen challenge. The efficiency of Treg cell depletion, as judged by using flow cytometric analysis of the residual GFP<sup>+</sup>CD4<sup>+</sup> T-cell populations, was greater than 80% in the lung and MLNs, even when assessed 3 days after application of the last

DT dose (see Fig E5, A and B, in this article's Online Repository at [www.jacionline.org](http://www.jacionline.org)). The beneficial effects of perinatal exposure to *H pylori* extract on allergen-induced bronchoalveolar infiltration and eosinophilia and on pulmonary inflammation and goblet cell metaplasia were largely abolished by Treg cell depletion (Fig 5), as were the effects on HDM-specific serum IgE titers and the pulmonary expression of the T<sub>H</sub>2 cytokine IL-13 (see Fig E5, C and D). In line with a previous report,<sup>34</sup> Treg cell depletion aggravated pulmonary inflammation and goblet cell metaplasia but not airway eosinophilia also in mock-treated Foxp3<sup>DTR</sup> mice of the positive control group (Fig 5). Furthermore, the same readouts showed a (although not significant) trend toward lower allergy even in transmaternally *H pylori*-exposed mice that were depleted of their Treg cells, indicating that Treg cell-independent regulatory pathways might contribute to the reduction in allergy symptoms that is a hallmark of



transmaternally exposed animals. The combined results implicate Treg cells in suppression of excessive allergen-specific immune responses in both transmaternally exposed and mock-treated offspring.

### Perinatal extract and VacA treatment result in enhanced demethylation of the TSDR in Foxp3<sup>+</sup> Treg cells and a specific transcriptional profile

Treg cells contribute to allergy protection in mice that are perinatally tolerized with *H pylori* extract or VacA (Fig 5), and the frequencies of specific Treg cell subsets are increased in the lungs as a consequence of the treatment (Fig 3). Therefore we set out to assess whether the same interventions affect the epigenetic processes driving the differentiation and stability of Treg cells.

To this end, we quantified the methylation status of CpG motifs (Fig 6, A) localized within an intronic enhancer region of the *Foxp3* locus termed TSDR because of its selective demethylation in lineage-committed (stable) Treg cells.<sup>35,36</sup> Treg cells from pooled MLNs of 5 to 10 male adult mice per group were FACS sorted based on their CD4 and Foxp3 expression and subjected to genomic DNA extraction, bisulfite conversion, and TSDR-specific pyrosequencing. CD4<sup>+</sup>Foxp3<sup>+</sup> T cells were sorted and analyzed in parallel. We used MLN Treg cells because the cell numbers that were obtained from the lungs were far too low for methylation analyses. As expected, Foxp3<sup>+</sup> T cells exhibited a demethylated TSDR, with approximately 95% methylated CpG motifs (Fig 6, B); their methylation did not change on intervention (data not shown). In contrast, Foxp3<sup>+</sup> T cells exhibited strong differences in methylation status. Although Foxp3<sup>+</sup> T cells that had been harvested from naive mice showed methylation levels varying between 25% and 40% depending on the experiment, this level was reduced to 5% to 15% because of perinatal intervention with extract or VacA (Fig 6, B). The 10 analyzed CpG motifs of the TSDR showed very consistent methylation patterns within 1 sample, indicating an all-or-nothing mechanism of demethylation that encompasses the entire locus (note that not all regions could be analyzed in all samples; Fig 6, B). Furthermore, a quantitative RT-PCR-based analysis of the Treg cell-specific transcripts FoxP3, IL-10, and TGF- $\beta$  conducted on CD4<sup>+</sup>Foxp3<sup>+</sup> Treg cells sorted in parallel from lungs and MLNs showed modestly higher TGF- $\beta$  but not Foxp3 and IL-10 expression because of the 2 interventions (see Fig E6, A and B, in this article's Online Repository at [www.jacionline.org](http://www.jacionline.org)).

To obtain a more comprehensive picture of differential gene expression in pulmonary Treg cells from extract- versus PBS-treated mice, we performed RNA sequencing on 2 extract-

and 3 PBS-treated pools of 20,000 CD4<sup>+</sup>Foxp3<sup>+</sup> Treg cells each (combined from 3-4 mice per pool; see Fig E6, C-E; Gene Expression Omnibus accession no. GSE116116). We found the samples to segregate based on treatment if the 2,000 most differentially expressed genes were used for unbiased clustering (see Fig E6, C); 248 genes were significantly differentially expressed in the 2 treatment groups, with a fold change cutoff log ratio of greater than 0.5 and *P* value of less than .01, with the majority of transcripts showing greater expression in extract-treated relative to control Treg cells (see Fig E6, D). Among the differentially expressed genes were genes of the TGF- $\beta$  signaling pathway (*Tgfb1* and *Smad3*), the IL-10 receptor  $\alpha$  chain (*Il10ra*), several genes that had previously been linked to Treg cells found in visceral adipose tissue (*Ccr1* and *Cd36*), and several genes known to be involved in Treg cell functionality and suppressive activity (*Themis2* and *Runx3*; see Fig E6, E).<sup>37-39</sup> We conclude from these data that epigenetic marks leading to stable expression of Foxp3 and the definitive lineage commitment of Treg cells, along with differential gene expression caused by extract exposure, reflect and likely mediate the suppressive effects of *H pylori*-specific perinatal interventions on allergic airway inflammation.

### Decreased susceptibility to allergic airway inflammation by means of exposure to *H pylori* extract is intergenerationally transmitted to the F2 generation

Enhanced demethylation of the TSDR in Foxp3<sup>+</sup> Treg cells from extract- and VacA-treated mice encouraged us to set up additional crosses, this time between perinatally extract-exposed (ie, through oral gavage of their mothers) and naive offspring. Strikingly, we found that the severity of HDM-induced allergic airway inflammation, goblet cell metaplasia, and eosinophilia was reduced (although not significantly in all readouts), even in the F2 generation born to perinatally extract-exposed offspring, which are grandchildren of extract-treated dams (Fig 7, A-E). It did not matter in this context whether only the father, only the mother, or both parents of HDM-sensitized and challenged offspring had been exposed *in utero* and during lactation to the *H pylori* extract administered to their mother (Fig 7). Also, both sexes exhibited similar levels of protection, arguing that non-X-chromosome-encoded regions other than the TSDR might be involved in such intergenerational protective effects. Interestingly, immunophenotyping analyses of the pulmonary Treg cell compartment of F2 mice revealed similar differences, as observed in the (protected) F1 generation (Fig 7, F-I). Although

**FIG 7.** *H pylori* extract induces intergenerational protection against allergic airway inflammation and skews lung T-cell responses of the F2 generation. F0 dams were subjected to twice-weekly oral gavage with *H pylori* extract (*H.p. extr*) or PBS during pregnancy and lactation. Perinatally exposed F1 animals obtained in this manner were bred with each other or with naive mates. At 6 weeks of age, F2 progeny were subjected to flow cytometric analysis of the pulmonary T-cell compartment (F-I) or sensitized and challenged (*s/c*) intranasally with HDM allergen (A-E). Fig 7, A, Total leukocytes in 1 mL of bronchoalveolar lavage fluid (BALF). Fig 7, B, Total eosinophils in 1 mL of BALF. Fig 7, C, Eosinophil frequencies in BALF. Fig 7, D and E, Pulmonary inflammation and goblet cell metaplasia. Fig 7, F, Foxp3<sup>+</sup> Treg cell frequencies among all T cells. Fig 7, G, Peripherally induced Treg (*pTreg*) cells (Nrp-1<sup>-</sup>) frequencies among all Foxp3<sup>+</sup> Treg cells. Fig 7, H and I, Frequencies of Cxcr3<sup>+</sup> and ROR $\gamma$ <sup>+</sup> Treg cells among all CD4<sup>+</sup>FoxP3<sup>+</sup> Treg cells. Each symbol represents 1 mouse. Results were pooled from 3 (Fig 7, A-E) or 2 (Fig 7, F-I) independent experiments. In Fig 7, A-E, ANOVA with Dunn multiple comparison correction was used for calculation of *P* values. In Fig 7, F-I, an unpaired Mann-Whitney *U* test was used for calculation of *P* values. \**P* < .05, \*\**P* < .01, and \*\*\*\**P* < .0001. *n.s.*, Not significant.

overall Foxp3<sup>+</sup> Treg cell frequencies did not differ significantly among the 2 treatment groups, extract-exposed mice exhibited higher frequencies of pulmonary neuropilin-negative peripherally induced Treg cells and CXCR3<sup>+</sup> and RORγt<sup>+</sup> Treg cell subsets (Fig 7, F-I). In contrast, IRF4<sup>+</sup> Treg cells were underrepresented in the lungs of extract-exposed mice (data not shown).

These experiments do not rule out that the F2 offspring benefited in terms of their reduced allergy severity because the gametes that form in the developing fetus *in utero* had been exposed to the tolerance-promoting components of *H pylori* extract. Indeed, further interbreeding of F2 offspring with one another yielded a generation of mice (F3) that showed no evidence of protection whatsoever (see Fig E7 in this article's Online Repository at [www.jacionline.org](http://www.jacionline.org)), indicating that the protective effects of this type of environmental exposure are limited to directly exposed generations.

## DISCUSSION

In this study we present the first experimental evidence for an intergenerational effect of perinatal exposure to *H pylori*-derived immunomodulatory molecules during pregnancy and lactation on several parameters of atopic sensitization and allergen-induced airway inflammation. We further report several immunologic, meta-genomic, and epigenetic correlates of perinatal *H pylori* exposure that might at least partly account for the observed protective effects. Acquisition of *H pylori* in early life has been implicated in epidemiologic and experimental studies in having a clearly detectable influence on allergy risk and severity, especially in children and young adults and their murine counterparts in experimental models of allergic airway inflammation.<sup>12-19</sup> Here we have extended these findings and focused on possible exposures occurring even earlier in life (ie, *in utero* and during lactation).

To exclude the risk of vertical transmission of the infection from mother to offspring, a route that has been identified as the main route of *H pylori* transmission in human subjects,<sup>40</sup> we instead opted to treat pregnant or lactating dams with *H pylori* extract or purified VacA, the main immunomodulatory molecule secreted by *H pylori* that is known to skew T-cell responses toward Treg cells and promote persistent colonization.<sup>18</sup> Interestingly, we found that direct transmaternal exposure to *H pylori* components, either *in utero* or during lactation, was required because discontinuation of the treatment of the (prospective) mother before mating did not confer protection. This finding argues that immunomodulatory molecules produced by *H pylori*, rather than tolerance-promoting factors produced by the mother, confer protection to the offspring.

The concept that direct perinatal exposure to specific intact microbes might be beneficial with respect to allergy risk and severity has been tested in experimental models with bacteria isolated from the farming environment, such as *Acinetobacter lwoffii*, *Lactobacillus lactis*, *Bacillus licheniformis*, and *Staphylococcus sciuri*.<sup>3,41-43</sup> Transmaternal allergy-protective effects, as shown here for *H pylori* (with exposure occurring exclusively through the mother), were reported in experimental models with *A lwoffii* and in those models were dependent on intact Toll-like receptor signaling and IL-6, TNF-α, and IL-12 production in the mother and epigenetically regulated IFN-γ production in the offspring.<sup>44,45</sup> Observational studies in human subjects lend further support to the idea that prenatal microbial

exposures (eg, to farming environments) have extensive effects on innate and adaptive immune function that are regulated at least in part through epigenetic mechanisms.<sup>46,47</sup> Treg cells have been implicated in some of the benefits associated with prenatal exposure (through the mother) to farming environments; their numbers and functionality in cord blood were found to be significantly greater in offspring of farm-exposed relative to control mothers, which in turn was associated with lower T<sub>H</sub>2 cytokine secretion and lymphoproliferation on innate stimulation.<sup>46</sup> Conversely, reduced Foxp3 expression in fetus-derived placental tissues appears to predict allergic disease in infancy.<sup>47</sup>

Three pieces of evidence implicate Foxp3<sup>+</sup> Treg cells in the beneficial effects of perinatal transmaternal exposure to *H pylori* and its immunomodulator VacA. On the one hand, we observe in the steady state (ie, before allergen sensitization and challenge) that the frequencies of specific Treg cell subsets, all of which are associated with particularly strong suppressive activities,<sup>29-32</sup> in the lung are greater than those without such perinatal exposure. Second, we detected enhanced demethylation of the TSDR within the *Foxp3* locus, which serves as an indicator of stable and irreversible differentiation toward the Treg cell lineage,<sup>35,36</sup> only in Treg cells from *H pylori*-exposed but not naive mice. Finally, the specific and selective depletion of Foxp3<sup>+</sup> Treg cells by means of DT administration during the challenge phase of the allergy protocol abrogates the benefits of transmaternal exposure, indicating that suppression of allergen-specific T<sub>H</sub>2 responses (and their signature cytokines, as determined in this study for IL-5 and IL-13) is driven by Treg cells. The greater infiltration of *H pylori*-exposed lungs with certain subsets of Treg cells in the steady state correlates well with their lower T-effector cell frequencies; the preferential priming (or local expansion) of Treg cells over effector T cells might be attributable to the skewed ratio of DCs with tolerogenic versus inflammatory activities.

The CD103<sup>+</sup> DCs that are overrepresented in the lungs of *H pylori*-exposed mice relative to CD11b<sup>+</sup> DCs depend on the transcription factor basic leucine zipper ATF-like 3 (BATF3) and are known for their potency in driving CD8<sup>+</sup> T-cell immunity<sup>48-50</sup> and for their role in priming Treg cell differentiation through production of retinoic acid.<sup>51,52</sup> Although their exclusive and nonredundant role in promoting Treg cell-driven tolerance was recently questioned in an oral tolerization model,<sup>53</sup> we have found their overrepresentation in the lung to be indicative of protection against airway inflammation in experimental models.<sup>22</sup> Furthermore, deficiency of CD103<sup>+</sup> DCs in *Batf3*<sup>-/-</sup> mice abrogates the protective effects of live infection<sup>22</sup> and also of direct VacA treatment (unpublished data). More work will be required to elucidate which of the various differentially represented Treg cell subsets depend on CD103<sup>+</sup> DCs for their priming or local expansion and whether BATF3 proficiency is required for protection of transmaternally exposed offspring to allergic airway inflammation.

We found 3 Treg cell subsets to be overrepresented in the lungs of *H pylori*-exposed animals despite similar overall Foxp3<sup>+</sup> Treg cell frequencies. These were Nrp1<sup>-</sup> Treg cells (ie, cells that presumably arose in the periphery in a thymus-independent manner), as well as RORγt<sup>+</sup> and CXCR3<sup>+</sup> subsets of both peripherally induced Treg cells and, to a lesser extent, thymus-dependent natural Treg cells. Notably, in contrast to the gastrointestinal tract,<sup>32</sup> we found that RORγt and CXCR3 were not generally coexpressed in the pulmonary Treg cell compartment. Expression of the chemokine receptor CXCR3 is

known to be driven by T-box transcription factor (T-bet) and can be used as a marker of cells that have at some stage of their ontogeny (transiently or stably) expressed T-bet.<sup>32</sup> T-bet-dependent CXCR3<sup>+</sup> Treg cells have recently been shown to develop in parallel to T-bet<sup>+</sup> T<sub>H</sub>1 cells during infection with *Listeria monocytogenes*,<sup>32</sup> which, similar to *H pylori*, is a strong T<sub>H</sub>1 inducer. Furthermore, loss of T-bet<sup>+</sup> Treg cells (through selective depletion of Foxp3 expression in T-bet<sup>+</sup> Treg cells) is sufficient to induce systemic autoimmunity, notably with strong T-effector cell infiltration into the lung.<sup>32</sup>

Our immunophenotyping data, although largely descriptive, are consistent with the novel concept that Treg cells coexpressing Foxp3 and T-bet/CXCR3 have an essential immunosuppressive function and further suggest that not only autoimmunity but also T<sub>H</sub>2-driven allergy is controlled by these cells. In contrast, we found IRF4<sup>+</sup> Treg cells to be underrepresented rather than overrepresented in the lungs of *H pylori*-exposed animals, largely as a consequence of the increased frequencies of the other 2 (RORγt<sup>+</sup> and CXCR3<sup>+</sup>) populations. Because IRF4 expression in Treg cells had previously been shown to endow these cells with the ability to selectively suppress T<sub>H</sub>2 responses,<sup>54</sup> we expected numbers of IRF4<sup>+</sup> Treg cells to increase in the setting of perinatal *H pylori* exposure; however, this was not the case.

Interestingly, the observed shifts in immune cell populations that are a hallmark of mice transmaternally exposed to *H pylori* did not affect antiviral responses, which were normal in a model of pulmonary influenza infection, as well as in a model of intestinal *C rodentium* infection. We further speculated that the differences in CD4<sup>+</sup> T-cell populations, in particular those affecting effector T/Treg cell ratios, would have an influence on microbial communities in the upper airways, as well as the gastrointestinal tract. Indeed, we found both transmaternal VacA and *H pylori* extract exposure to measurably affect microbial communities in all examined sites of the gastrointestinal tract. An unbiased analysis of community composition revealed largely distinct, nonoverlapping changes caused by treatment with extract and VacA, respectively; however, among the significant changes in relative abundance of individual taxonomic units that were detected, quite a few were found to occur with both VacA and extract treatment (eg, depletion of Firmicutes and Bacteroidetes in the stomach and depletion of *Akkermansia* and *Desulfovibrio* species in the ileum). Although the described cecal transplantation experiments appear to rule out a causal role for the altered microbiota composition in preventing allergic airway inflammation, we found it interesting that some of the shifts occurred in taxa that have previously been associated with healthy versus diseased states, such as segmented filamentous bacteria.

The most striking observation made in the course of our studies related to the intergenerational transmission of allergy protection. Such effects had been reported mostly for exposure to tobacco smoke, where not only maternal but also grandmaternal smoking is associated with increased risk for childhood asthma in human subjects.<sup>55</sup> Results of the observational studies in human subjects have been corroborated in a rat model of nicotine-induced asthma, in which a transgenerational transmission to the F2 and F3 generations could be demonstrated after perinatal nicotine exposure of F0 dams.<sup>56</sup>

Collectively, our findings indicate that transmaternal prenatal and postnatal exposure to *H pylori* and its main immunomodulator VacA has suppressive effects on the severity of allergic airway inflammation later in life, which likely is

attributable to the suppressive activity of the pulmonary Treg cells that are induced under such conditions.

Our study has 3 major limitations; on the one hand, we provide only descriptive and not functional evidence of the suppressive role of pulmonary RORγt<sup>+</sup> and CXCR3<sup>+</sup> Treg cells in airway inflammation. Second, we have not conducted methacholine assays because of the technical challenges associated with this procedure and therefore cannot judge the effects on lung function of perinatal exposure to *H pylori*. Finally, the negative data obtained on cecal transplantation do not definitively rule out that shifts in the gastrointestinal microbiota contribute to the effects of perinatal tolerization with *H pylori*. Additional experiments to this end could involve cohousing or antibiotic pretreatment before cecal transplantation in an effort to improve the colonization of transplanted communities.

Among the useful indicators of the reduced allergy risk associated with perinatal *H pylori* exposure are shifts in the microbiota composition of various sites of the gastrointestinal tract, as well as the epigenetic signature of the *Foxp3* locus, which indicates qualitative or at least quantitative differences in the stability and functionality of Treg cells because of this treatment. Importantly, perinatal exposure to *H pylori* does not result in generalized immunosuppression and increased susceptibility to viral or bacterial infection; rather, acute infection with the lung pathogen IAV or with the gastrointestinal pathogen *C rodentium* readily breaks perinatally induced immune tolerance. We propose that the common human amphibiont *H pylori* functions as an integral part of the early-life “exposome” that skews the developing immune system toward immune tolerance.

#### Key messages

- **Transmaternal exposure to *H pylori* reduces allergic airway inflammation in F1 and F2 offspring.**
- **Protection against allergy requires Treg cells and is associated with robust shifts in the gastrointestinal microbiota but not general immunosuppression.**
- **Analysis of lung T-cell and DC subsets reveals immunologic correlates of allergy protection.**

#### REFERENCES

1. WHO Asthma Fact Sheet. Available at: <http://www.who.int/mediacentre/factsheets/fs307/en/>. Accessed October 9, 2018.
2. Kyburz A, Muller A. The gastrointestinal tract microbiota and allergic diseases. *Dig Dis* 2016;34:230-43.
3. Renz H, Holt PG, Inouye M, Logan AC, Prescott SL, Sly PD. An exposome perspective: early-life events and immune development in a changing world. *J Allergy Clin Immunol* 2017;140:24-40.
4. Braun-Fahrlander C, Riedler J, Herz U, Eder W, Waser M, Grize L, et al. Environmental exposure to endotoxin and its relation to asthma in school-age children. *N Engl J Med* 2002;347:869-77.
5. Ege MJ, Bieli C, Frei R, van Strien RT, Riedler J, Ublagger E, et al. Prenatal farm exposure is related to the expression of receptors of the innate immunity and to atopic sensitization in school-age children. *J Allergy Clin Immunol* 2006;117:817-23.
6. Rautava S, Luoto R, Salminen S, Isolauri E. Microbial contact during pregnancy, intestinal colonization and human disease. *Nat Rev Gastroenterol Hepatol* 2012;9:565-76.
7. West CE. Gut microbiota and allergic disease: new findings. *Curr Opin Clin Nutr Metab Care* 2014;17:261-6.
8. West CE, Jenmalm MC, Prescott SL. The gut microbiota and its role in the development of allergic disease: a wider perspective. *Clin Exp Allergy* 2015;45:43-53.

9. Dominguez-Bello MG, Costello EK, Contreras M, Magris M, Hidalgo G, Fierer N, et al. Delivery mode shapes the acquisition and structure of the initial microbiota across multiple body habitats in newborns. *Proc Natl Acad Sci U S A* 2010;107:11971-5.
10. Alcantara-Neves NM, de SGBG, Veiga RV, Figueiredo CA, Fiaccone RL, da Conceicao JS, et al. Effects of helminth co-infections on atopy, asthma and cytokine production in children living in a poor urban area in Latin America. *BMC Res Notes* 2014;7:817.
11. Ponte EV, Rasella D, Souza-Machado C, Stelmach R, Barreto ML, Cruz AA. Reduced asthma morbidity in endemic areas for helminth infections: a longitudinal ecological study in Brazil. *J Asthma* 2014;51:1022-7.
12. Chen Y, Blaser MJ. Inverse associations of *Helicobacter pylori* with asthma and allergy. *Arch Intern Med* 2007;167:821-7.
13. Chen Y, Blaser MJ. *Helicobacter pylori* colonization is inversely associated with childhood asthma. *J Infect Dis* 2008;198:553-60.
14. Amberbir A, Medhin G, Abegaz WE, Hanlon C, Robinson K, Fogarty A, et al. Exposure to *Helicobacter pylori* infection in early childhood and the risk of allergic disease and atopic sensitization: a longitudinal birth cohort study. *Clin Exp Allergy* 2014;44:563-71.
15. Amberbir A, Medhin G, Erku W, Alem A, Simms R, Robinson K, et al. Effects of *Helicobacter pylori*, geohelminth infection and selected commensal bacteria on the risk of allergic disease and sensitization in 3-year-old Ethiopian children. *Clin Exp Allergy* 2011;41:1422-30.
16. Arnold IC, Dehzad N, Reuter S, Martin H, Becher B, Taube C, et al. *Helicobacter pylori* infection prevents allergic asthma in mouse models through the induction of regulatory T cells. *J Clin Invest* 2011;121:3088-93.
17. Koch KN, Hartung ML, Urban S, Kyburz A, Bahlmann AS, Lind J, et al. *Helicobacter urease*-induced activation of the TLR2/NLRP3/IL-18 axis protects against asthma. *J Clin Invest* 2015;125:3297-302.
18. Oertli M, Noben M, Engler DB, Semper RP, Reuter S, Maxeiner J, et al. *Helicobacter pylori* gamma-glutamyl transpeptidase and vacuolating cytotoxin promote gastric persistence and immune tolerance. *Proc Natl Acad Sci U S A* 2013;110:3047-52.
19. Oertli M, Sundquist M, Hitzler I, Engler DB, Arnold IC, Reuter S, et al. DC-derived IL-18 drives Treg differentiation, murine *Helicobacter pylori*-specific immune tolerance, and asthma protection. *J Clin Invest* 2012;122:1082-96.
20. Wang Q, Yu C, Sun Y. The association between asthma and *Helicobacter pylori*: a meta-analysis. *Helicobacter* 2013;18:41-53.
21. Zhou X, Wu J, Zhang G. Association between *Helicobacter pylori* and asthma: a meta-analysis. *Eur J Gastroenterol Hepatol* 2013;25:460-8.
22. Engler DB, Reuter S, van Wijck Y, Urban S, Kyburz A, Maxeiner J, et al. Effective treatment of allergic airway inflammation with *Helicobacter pylori* immunomodulators requires BATF3-dependent dendritic cells and IL-10. *Proc Natl Acad Sci U S A* 2014;111:11810-5.
23. Kabisch R, Semper RP, Wustner S, Gerhard M, Mejias-Luque R. *Helicobacter pylori* gamma-glutamyltranspeptidase induces tolerogenic human dendritic cells by activation of glutamate receptors. *J Immunol* 2016;196:4246-52.
24. Gonzalez-Rivera C, Campbell AM, Rutherford SA, Pyburn TM, Foegeding NJ, Barke TL, et al. A nonoligomerizing mutant form of *Helicobacter pylori* VacA allows structural analysis of the p33 domain. *Infect Immun* 2016;84:2662-70.
25. Yang BH, Hagemann S, Mamareli P, Lauer U, Hoffmann U, Beckstette M, et al. Foxp3(+) T cells expressing ROR gamma t represent a stable regulatory T-cell effector lineage with enhanced suppressive capacity during intestinal inflammation. *Mucosal Immunol* 2016;9:444-57.
26. Caporaso JG, Lauber CL, Walters WA, Berg-Lyons D, Huntley J, Fierer N, et al. Ultra-high-throughput microbial community analysis on the Illumina HiSeq and MiSeq platforms. *ISME J* 2012;6:1621-4.
27. Kenney AD, Dowdle JA, Bozzacco L, McMichael TM, St Gelais C, Panfil AR, et al. Human genetic determinants of viral diseases. *Annu Rev Genet* 2017;51:241-63.
28. Kyburz A, Urban S, Altobelli A, Floess S, Huehn J, Cover TL, et al. *Helicobacter pylori* and its secreted immunomodulator VacA protect against anaphylaxis in experimental models of food allergy. *Clin Exp Allergy* 2017;47:1331-41.
29. Koch MA, Tucker-Heard G, Perdue NR, Killebrew JR, Urdahl KB, Campbell DJ. The transcription factor T-bet controls regulatory T cell homeostasis and function during type 1 inflammation. *Nat Immunol* 2009;10:595-602.
30. Ohnmacht C, Park JH, Cording S, Wing JB, Atarashi K, Obata Y, et al. Mucosal immunology. The microbiota regulates type 2 immunity through RORgamma(+) T cells. *Science* 2015;349:989-93.
31. Sefik E, Geva-Zatorsky N, Oh S, Konnikova L, Zemmour D, McGuire AM, et al. Mucosal immunology. Individual intestinal symbionts induce a distinct population of RORgamma(+) regulatory T cells. *Science* 2015;349:993-7.
32. Levine AG, Medoza A, Hemmers S, Moltedo B, Niec RE, Schizas M, et al. Stability and function of regulatory T cells expressing the transcription factor T-bet. *Nature* 2017;546:421-5.
33. Kim JM, Rasmussen JP, Rudensky AY. Regulatory T cells prevent catastrophic autoimmunity throughout the lifespan of mice. *Nat Immunol* 2007;8:191-7.
34. Baru AM, Hartl A, Lahl K, Krishnaswamy JK, Fehrenbach H, Yildirim AO, et al. Selective depletion of Foxp3+ Treg during sensitization phase aggravates experimental allergic airway inflammation. *Eur J Immunol* 2010;40:2259-66.
35. Toker A, Engelbert D, Garg G, Polansky JK, Floess S, Miyao T, et al. Active demethylation of the Foxp3 locus leads to the generation of stable regulatory T cells within the thymus. *J Immunol* 2013;190:3180-8.
36. Polansky JK, Kretschmer K, Freyer J, Floess S, Garbe A, Baron U, et al. DNA methylation controls Foxp3 gene expression. *Eur J Immunol* 2008;38:1654-63.
37. Pedros C, Gaud G, Bernard I, Kassem S, Chabod M, Lagrange D, et al. An epistatic interaction between Themis1 and Vav1 modulates regulatory T cell function and inflammatory bowel disease development. *J Immunol* 2015;195:1608-16.
38. Sugai M, Aoki K, Osato M, Nambu Y, Ito K, Taketo MM, et al. Runx3 is required for full activation of regulatory T cells to prevent colitis-associated tumor formation. *J Immunol* 2011;186:6515-20.
39. Burzyn D, Benoist C, Mathis D. Regulatory T cells in nonlymphoid tissues. *Nat Immunol* 2013;14:1007-13.
40. Weyermann M, Rothenbacher D, Brenner H. Acquisition of *Helicobacter pylori* infection in early childhood: independent contributions of infected mothers, fathers, and siblings. *Am J Gastroenterol* 2009;104:182-9.
41. Debarry J, Garn H, Hanuszkiewicz A, Dickgreber N, Blumer N, von Mutius E, et al. *Acinetobacter lwoffii* and *Lactococcus lactis* strains isolated from farm cowsheds possess strong allergy-protective properties. *J Allergy Clin Immunol* 2007;119:1514-21.
42. Vogel K, Blumer N, Korhals M, Mittelstadt J, Garn H, Ege M, et al. Animal shed *Bacillus licheniformis* spores possess allergy-protective as well as inflammatory properties. *J Allergy Clin Immunol* 2008;122:307-12, e1-8.
43. Hagner S, Harb H, Zhao M, Stein K, Holst O, Ege MJ, et al. Farm-derived gram-positive bacterium *Staphylococcus sciuri* W620 prevents asthma phenotype in HDM- and OVA-exposed mice. *Allergy* 2013;68:322-9.
44. Brand S, Teich R, Dicke T, Harb H, Yildirim AO, Tost J, et al. Epigenetic regulation in murine offspring as a novel mechanism for transmaternal asthma protection induced by microbes. *J Allergy Clin Immunol* 2011;128:618-25, e1-7.
45. Conrad ML, Ferstl R, Teich R, Brand S, Blumer N, Yildirim AO, et al. Maternal TLR signaling is required for prenatal asthma protection by the nonpathogenic microbe *Acinetobacter lwoffii* F78. *J Exp Med* 2009;206:2869-77.
46. Schaub B, Liu J, Hoppler S, Schleich I, Huehn J, Olek S, et al. Maternal farm exposure modulates neonatal immune mechanisms through regulatory T cells. *J Allergy Clin Immunol* 2009;123:774-82, e5.
47. Prescott SL, Tulic M, Kumah AO, Richman T, Crook M, Martino D, et al. Reduced placental FOXP3 associated with subsequent infant allergic disease. *J Allergy Clin Immunol* 2011;128:886-7, e5.
48. Edelson BT, Kc W, Juang R, Kohyama M, Benoit LA, Klekotka PA, et al. Peripheral CD103+ dendritic cells form a unified subset developmentally related to CD8alpha+ conventional dendritic cells. *J Exp Med* 2010;207:823-36.
49. Bogunovic M, Ginhoux F, Helft J, Shang L, Hashimoto D, Greter M, et al. Origin of the lamina propria dendritic cell network. *Immunity* 2009;31:513-25.
50. Varol C, Vallon-Eberhard A, Elinav E, Aychek T, Shapira Y, Luche H, et al. Intestinal lamina propria dendritic cell subsets have different origin and functions. *Immunity* 2009;31:502-12.
51. Coombes JL, Siddiqui KR, Arancibia-Carcamo CV, Hall J, Sun CM, Belkaid Y, et al. A functionally specialized population of mucosal CD103+ DCs induces Foxp3+ regulatory T cells via a TGF-beta and retinoic acid-dependent mechanism. *J Exp Med* 2007;204:1757-64.
52. Joeris T, Muller-Luda K, Agace WW, Mowat AM. Diversity and functions of intestinal mononuclear phagocytes. *Mucosal Immunol* 2017;10:845-64.
53. Venenbergen S, van Berkel LA, du Pre MF, He J, Karrich JJ, Costes LM, et al. Colon tolerance develops in the iliac lymph nodes and can be established independent of CD103(+) dendritic cells. *Mucosal Immunol* 2016;9:894-906.
54. Zheng Y, Chaudhry A, Kas A, deRoos P, Kim JM, Chu TT, et al. Regulatory T-cell suppressor program co-opts transcription factor IRF4 to control T(H)2 responses. *Nature* 2009;458:351-6.
55. Li YF, Langholz B, Salam MT, Gilliland FD. Maternal and grandmaternal smoking patterns are associated with early childhood asthma. *Chest* 2005;127:1232-41.
56. Rehan VK, Liu J, Sakurai R, Torday JS. Perinatal nicotine-induced transgenerational asthma. *Am J Physiol Lung Cell Mol Physiol* 2013;305:L501-7.

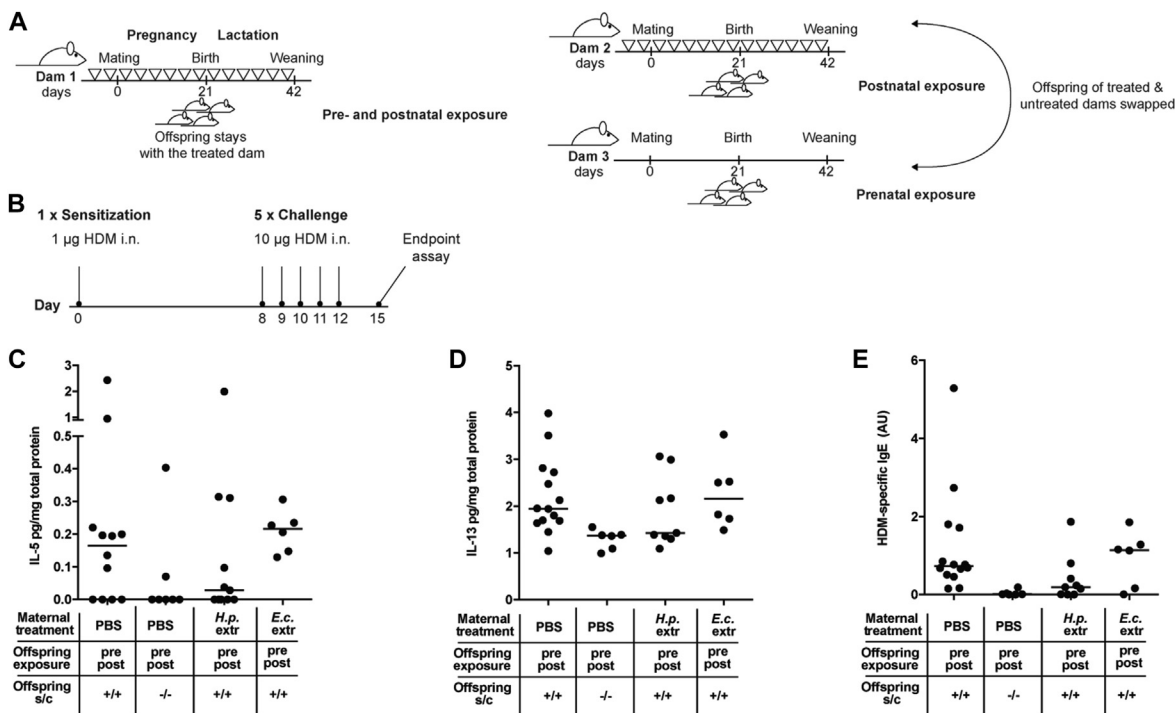


**FIG E1.** Perinatal transmaternal exposure to *H pylori* reduces HDM-induced allergic airway inflammation but does not induce generalized immunosuppression. **A** and **B**, Schematics in Fig E1, **A** and **B**, show the timeline of treatment of pregnant or lactating dams that was designed to generate offspring that were either prenatally and postnatally (dam 1) or prenatally or postnatally (dams 2 and 3) exposed to *H pylori* extract (Fig E1, **A**) and the protocol used throughout this study to induce allergic airway inflammation with HDM allergen (Fig E1, **B**). *i.n.*, Intranasal. **C-E**, Dams were treated orally twice weekly during pregnancy and lactation with the indicated bacterial extract. All offspring were sensitized and challenged (*s/c*) intranasally with HDM allergen at 6 weeks of age. Negative control mice were sensitized and challenged with PBS only. Fig E1, **C**, Pulmonary IL-5 expression, as assessed by using the chromatin bead array. Fig E1, **D**, IL-13 expression normalized to total protein content, as assessed by means of ELISA. Fig E1, **E**, HDM-specific IgE, as assessed by using serum ELISA, of mice shown in Fig 1. **F-J**, Mice were treated orally with *H pylori* extract or intraperitoneally with VacA from day 7 of life onward until the study end point; mice were additionally sensitized and challenged intranasally with HDM allergen, as described above. Bronchoalveolar lavage leukocytes and eosinophils were quantified at the study end point; lungs were fixed, hematoxylin and eosin or PAS stained, and scored with respect to peribronchiolar and perivascular inflammation and PAS<sup>+</sup> goblet cell metaplasia. Fig E1, **F**, Total leukocytes in 1 mL of bronchoalveolar lavage fluid (BALF). Fig E1, **G**, Total eosinophils in 1 mL of BALF. Fig E1, **H**, Eosinophil frequencies in BALF. **I** and **J**, Pulmonary inflammation and goblet cell metaplasia, as assessed on stained lung sections. **BM**, Basement membrane. Results shown in Fig E1, **F-J**, were pooled from 3 independent experiments. In Fig E1, **C-J**, each symbol represents 1 mouse. Horizontal lines indicate medians. **K-N**, Mice were prenatally and postnatally exposed to *H pylori* extract, as described above, and were infected intranasally with 200 pfu of IAV PR8 at 8 weeks of age. Fig E1, **K**, Weight plotted as a percentage of initial body weight on the day of infection. Fig E1, **L**, PR8-specific serum IgG titers, as detected by means of ELISA on day 9 after infection. Absorbance at 450 to 620 nm is plotted for serial dilutions of serum. Fig E1, **M**, High weight loss on day 8 after infection (plotted as percentage of initial weight) is directly correlated with high levels of anti-PR8 IgG in serum on day 9 after infection (plotted as absorbance at a dilution of 1:3200) for both experimental groups. Fig E1, **N**, IFN- $\gamma$  production by CD8<sup>+</sup> T cells, as detected by using intracellular cytokine staining and flow cytometric analysis of leukocytes that had been isolated from the lungs of infected mice on day 9 after infection and restimulated *in vitro* with PR8-specific peptides NP1<sub>366-374</sub> (dominant epitope) and HA<sub>211-225</sub> (subdominant epitope) or the irrelevant control peptide OVA<sub>257-264</sub>. The mean (+ SD) percentage of IFN- $\gamma$ -producing CD8<sup>+</sup> T cells for each specific epitope is plotted after subtraction of the percentage of nonspecific response to the irrelevant control peptide. PBS- and extract-treated groups each consist of 5 or 6 mice, respectively. Representative data of 1 uninfected animal are plotted alongside the infected mice. **O-Q**, Mice were prenatally and postnatally exposed to *H pylori* extract, as described above, and were infected orally with *C rodentium* for 12 days at 8 weeks of age. Colonic lamina propria preparations were subjected to multicolor flow cytometry. Frequencies of live CD45<sup>+</sup> cells, CD4<sup>+</sup> T cells, and CD8<sup>+</sup> T cells are shown in Fig E1, **O**; frequencies of IFN- $\gamma$ <sup>+</sup>, TNF- $\alpha$ <sup>+</sup>, and IL-17<sup>+</sup> T cells are shown in Fig E1, **P**, and colonic and cecal *C rodentium* burden, as assessed by plating on Luria broth plates supplemented with NAL and colony counting, is shown in Fig E1, **Q**. Bacterial loads were normalized to tissue weight. Each dot represents 1 animal throughout. ANOVA with the Dunn multiple comparisons test was used for calculation of *P* values. \*\**P* < .01 and \*\*\*\**P* < .0001. *n.s.*, Not significant.

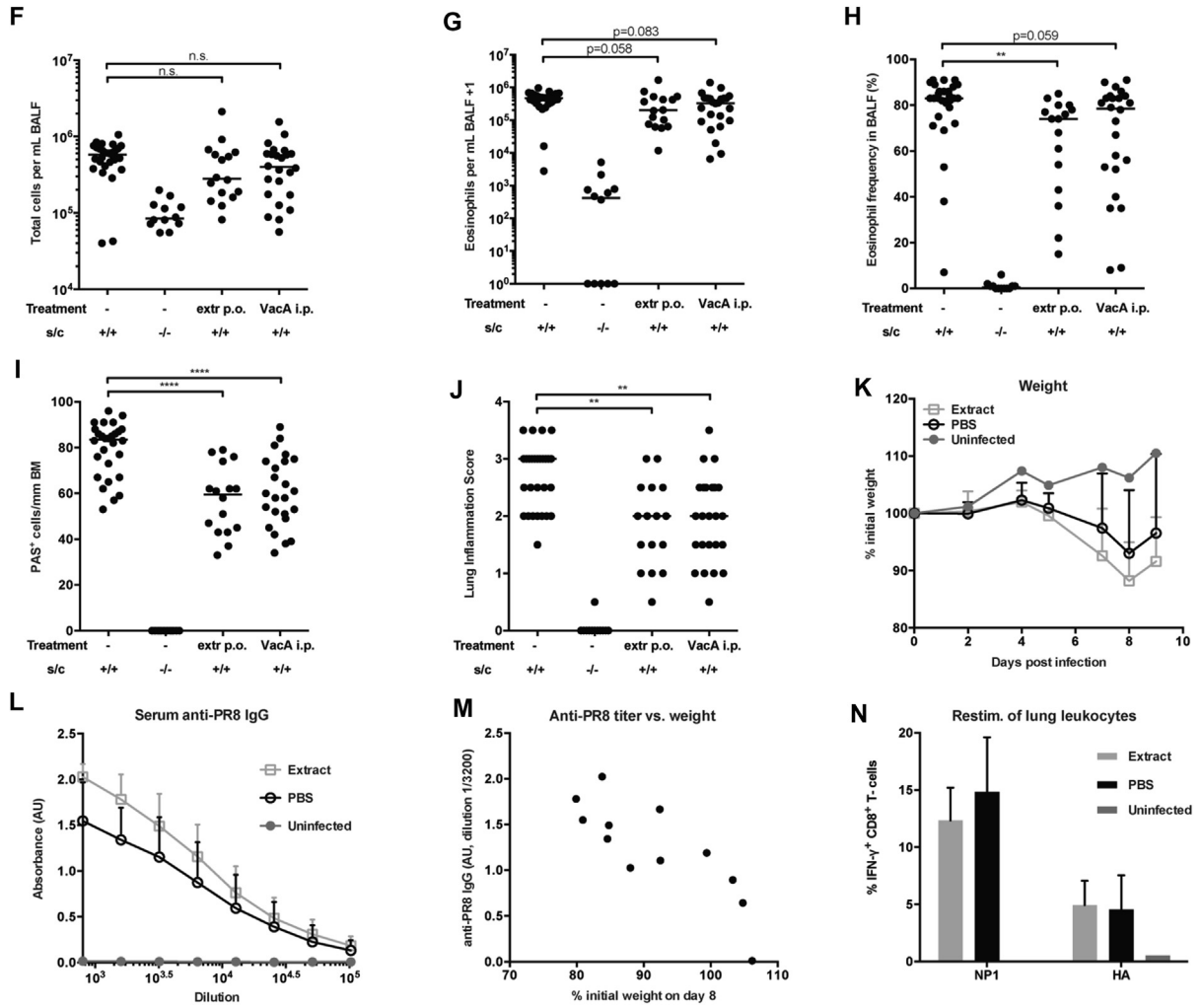


FIG E1. (Continued).

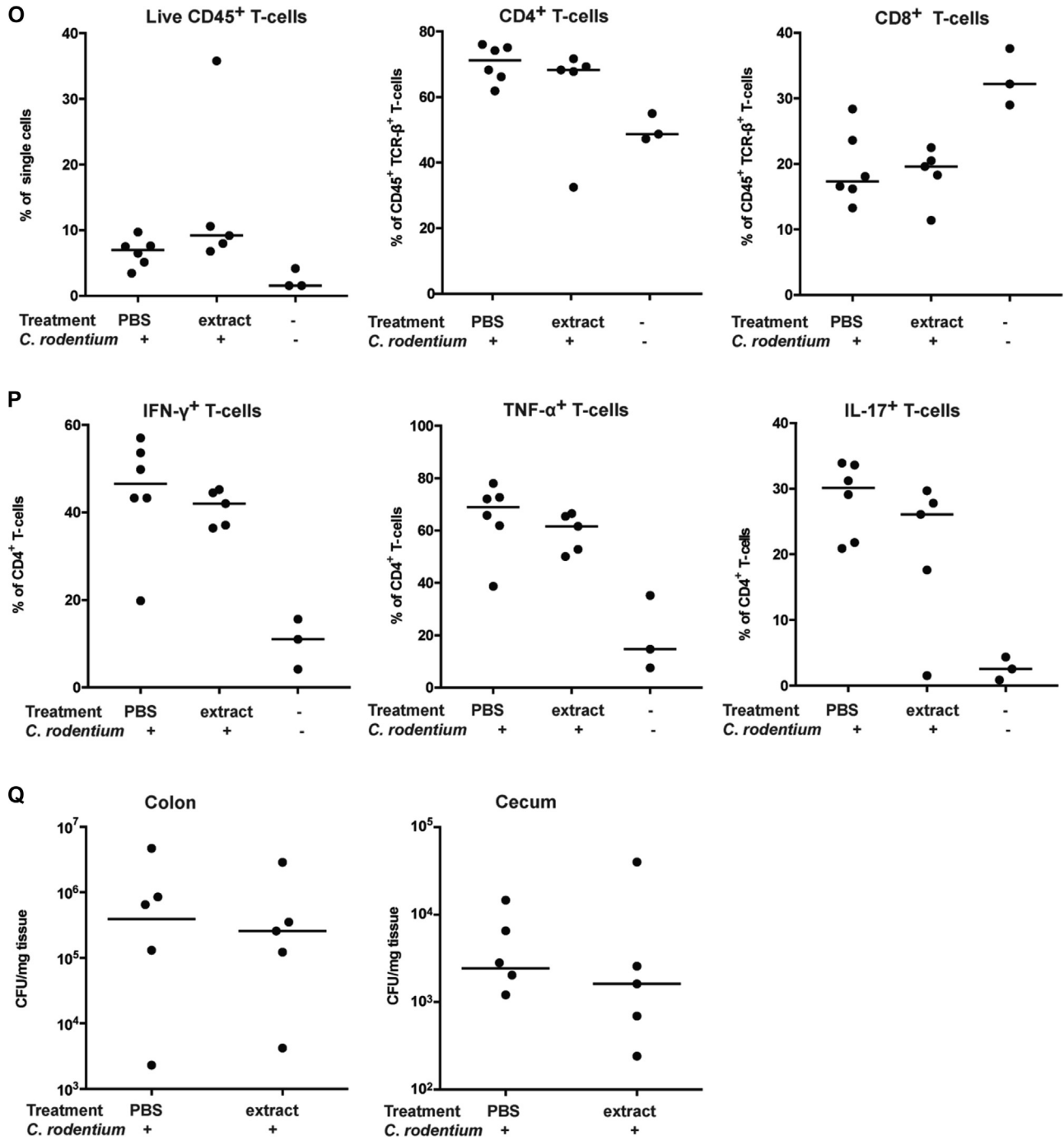
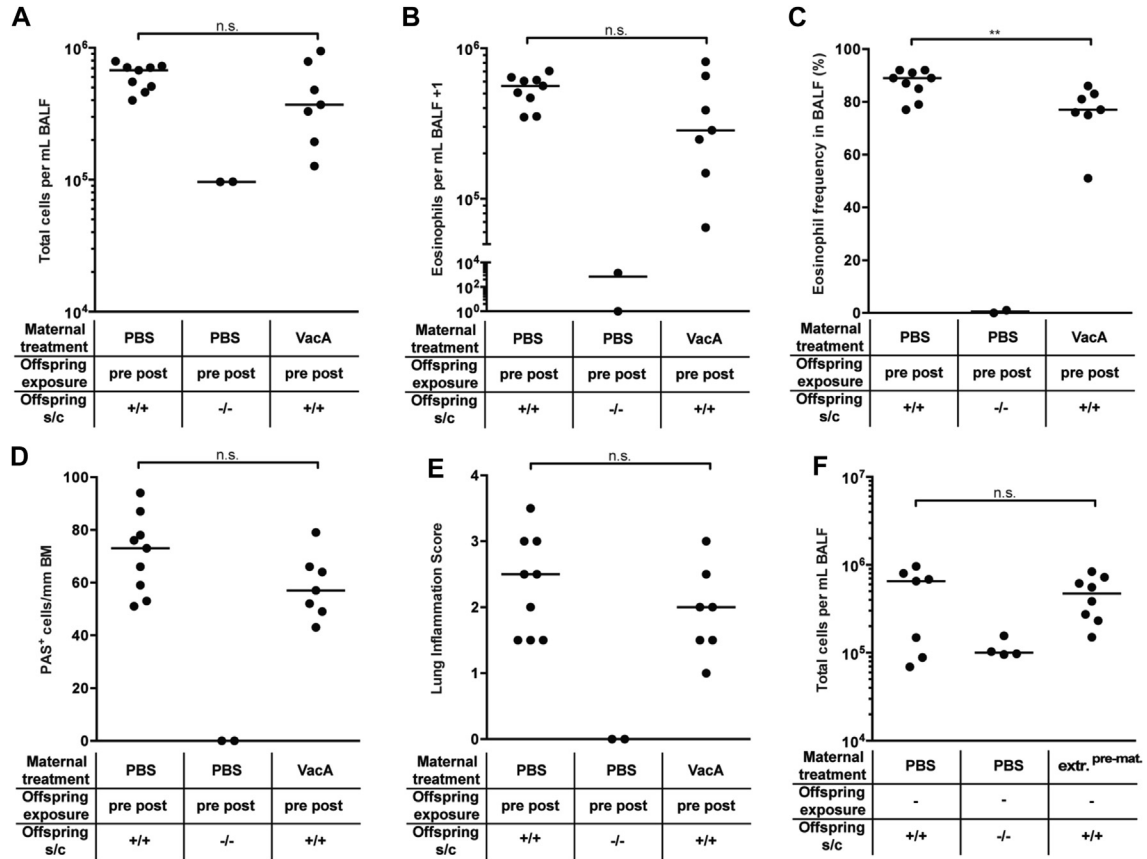


FIG E1. (Continued).



**FIG E2.** Prenatal and postnatal transmaternal exposure to *H pylori* VacA protects against HDM-induced allergic airway inflammation. **A-E**, Mice were prenatally and postnatally exposed to *H pylori* VacA through twice-weekly oral treatment of the dams with 20  $\mu$ g of purified VacA during pregnancy and lactation. Offspring of PBS-treated dams were used as control mice. At 6 weeks of age, offspring were sensitized and challenged (*s/c*) intranasally with HDM allergen. Negative control mice were sensitized and challenged with PBS only. Allergic airway inflammation was assessed as described in Fig 1. **A**, Total leukocytes in 1 mL of bronchoalveolar lavage fluid (BALF). **B**, Total eosinophils in 1 mL of BALF. **C**, Eosinophil frequencies in BALF. **D** and **E**, Pulmonary inflammation and goblet cell metaplasia, as assessed on stained lung sections. *BM*, basement membrane. **F-J**, Female mice were treated orally with *H pylori* extract from day 7 of life onward. At 7 weeks of age, treatment was discontinued, and female mice (extract-treated, pre-mating [*extr<sup>pre-mat</sup>*]) were bred with naive male mice to obtain offspring that were sensitized and challenged intranasally with HDM allergen at 6 weeks of age. Fig E2, **F**, Total leukocytes in 1 mL of BALF. Fig E2, **G**, Total eosinophils in 1 mL of BALF. Fig E2, **H**, Eosinophil frequencies in BALF. Fig E2, **I** and **J**, Pulmonary inflammation and goblet cell metaplasia, as assessed on stained lung sections. **K** and **L**, Mice were transmaternally prenatally and postnatally exposed to *H pylori* extract, as described in Fig 1. Mice were further sensitized and challenged with OVA to induce allergic airway inflammation. Goblet cell metaplasia and pulmonary inflammation, as assessed on stained lung sections, are shown in Fig E2, **K** and **L**; results are pooled from 2 independent experiments. Results in Fig E2, **A-E** and **F-J**, are from 1 experiment of each type. Horizontal lines indicate medians; the unpaired Mann-Whitney *U* test was used for statistical analyses. \*\**P* < .01 and \*\*\**P* < .001. *n.s.*, Not significant.

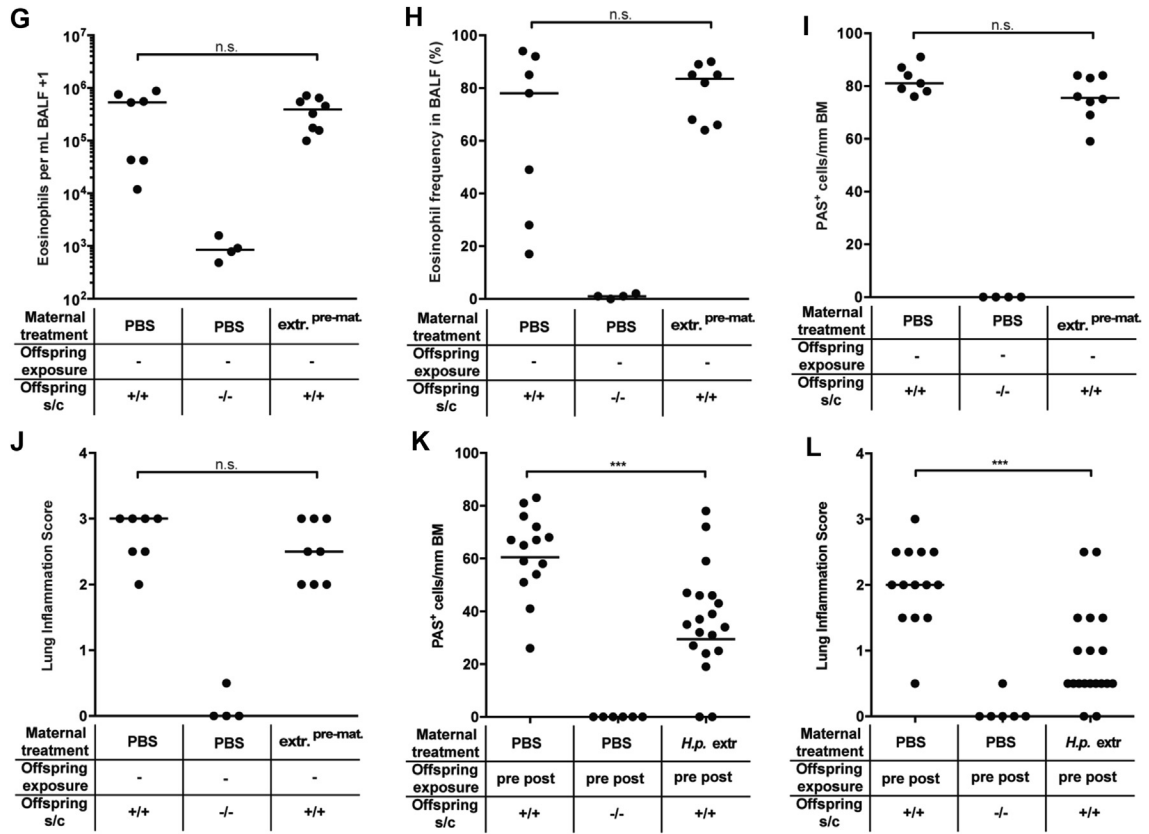
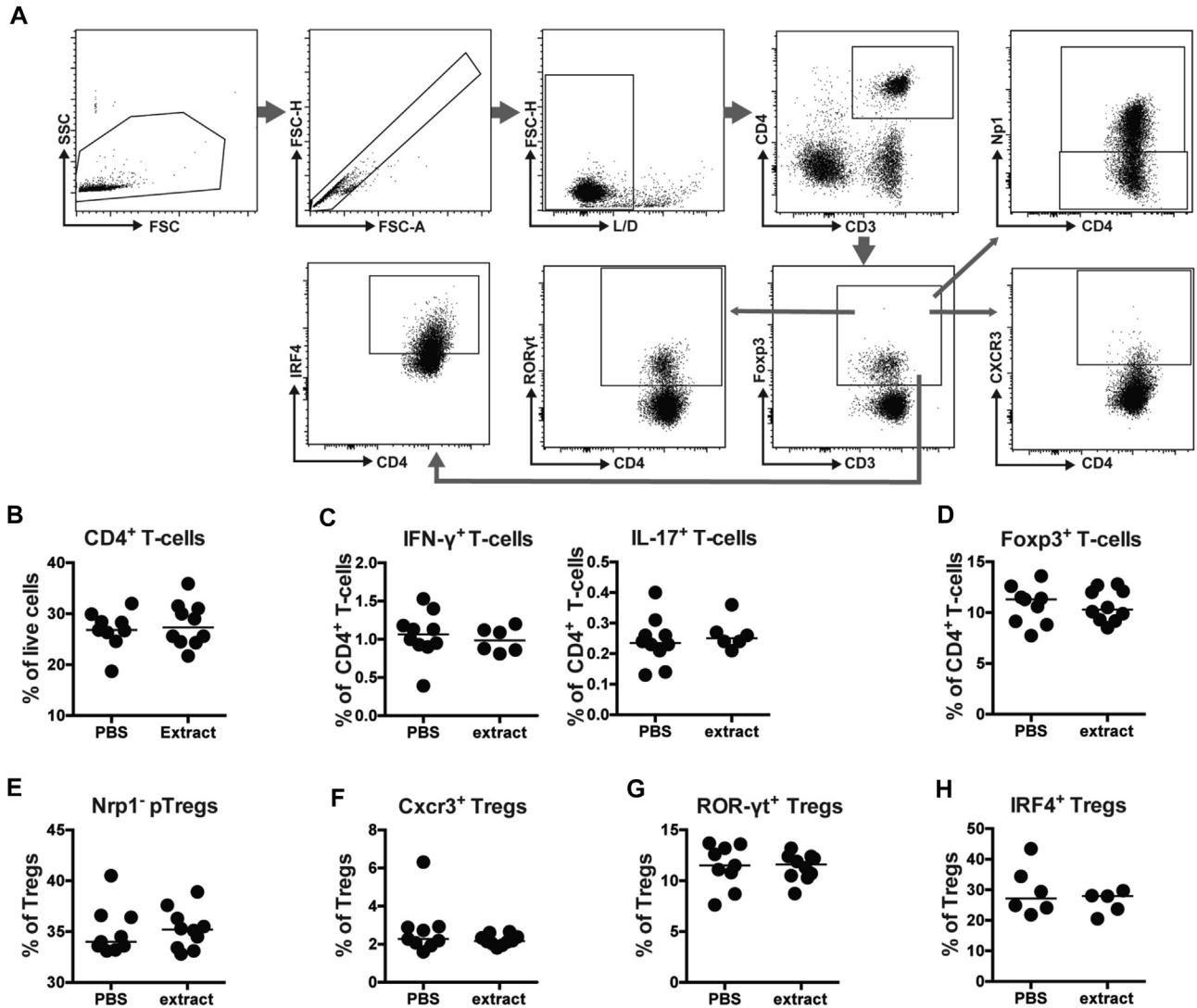


FIG E2. (Continued).



**FIG E3.** Perinatal transmaternal exposure to *H pylori* extract has no effect on Treg cell populations in the MLNs or on antigen processing and presentation by DCs. **A**, Gating strategy used for quantification of Treg cell subsets in Fig 3 and below. FSC, Forward scatter; SSC, side scatter. **B–M**, Mice were prenatally and postnatally exposed to *H pylori* extract or PBS through twice-weekly oral treatment of dams during pregnancy and lactation, as described in Fig 3. At 6 weeks of age, leukocytes were isolated from the lungs and, along with MLN T-cell and DC populations, were analyzed by using multicolor flow cytometry. For intracellular cytokine staining, leukocytes were restimulated *ex vivo* for 3 hours with phorbol 12-myristate 13-acetate/ionomycin. **B**, CD4<sup>+</sup> T-cell frequencies among all live MLN cells. **C**, T<sub>H</sub>1 and T<sub>H</sub>17 frequencies among all MLN CD4<sup>+</sup> T cells of the mice shown in Fig E3, B, and Fig 3. **D**, Foxp3<sup>+</sup> Treg cell frequencies in the MLNs of the mice shown in Fig E3, B, and Fig 3. **E–H**, Frequencies of the indicated Treg cell subsets among all MLN Foxp3<sup>+</sup> Treg cells. **I**, Frequencies of pulmonary CD103<sup>+</sup>CD11b<sup>+</sup> DCs. **J** and **K**, Frequencies of CD11c<sup>+</sup>MHCII<sup>high</sup> migratory DCs and CD11c<sup>+</sup>MHCII<sup>dim</sup> resident DCs among all CD45<sup>+</sup> MLN leukocytes. **L**, Ratios of CD103<sup>+</sup> over CD11b<sup>+</sup> migratory DCs. **M**, Ratios of CD8<sup>+</sup> over CD11b<sup>+</sup> resident DCs. Data in Fig E3, B–M, are pooled from 2 to 3 independent experiments, with the exception of Fig E3, H and I, which are from a single experiment representative of 2. **N–S**, Perinatally extract-exposed mice were intranasally challenged with 50  $\mu$ L of DQ-OVA (800  $\mu$ g/mL) and AF647-OVA (800  $\mu$ g/mL) approximately 15 hours before death and pulmonary leukocyte isolation. Fig E3, N and O, Frequencies of AF647<sup>+</sup> (Fig E3, N) and FITC<sup>+</sup> DCs (indicating processed DQ-OVA, which fluoresces in the FITC channel; Fig E3, O) among all CD11c<sup>+</sup> DCs. **P–S**, Frequencies of CD103<sup>−</sup>CD11b<sup>+</sup> and CD103<sup>−</sup>CD11b<sup>−</sup> DC subsets among all AF647<sup>+</sup> DCs (Fig E3, P and Q) or all DQ<sup>+</sup> (FITC<sup>+</sup>) DCs (Fig E3, R and S). Data in Fig E3, N–S, are from 1 experiment but representative of 2 independently conducted experiments.

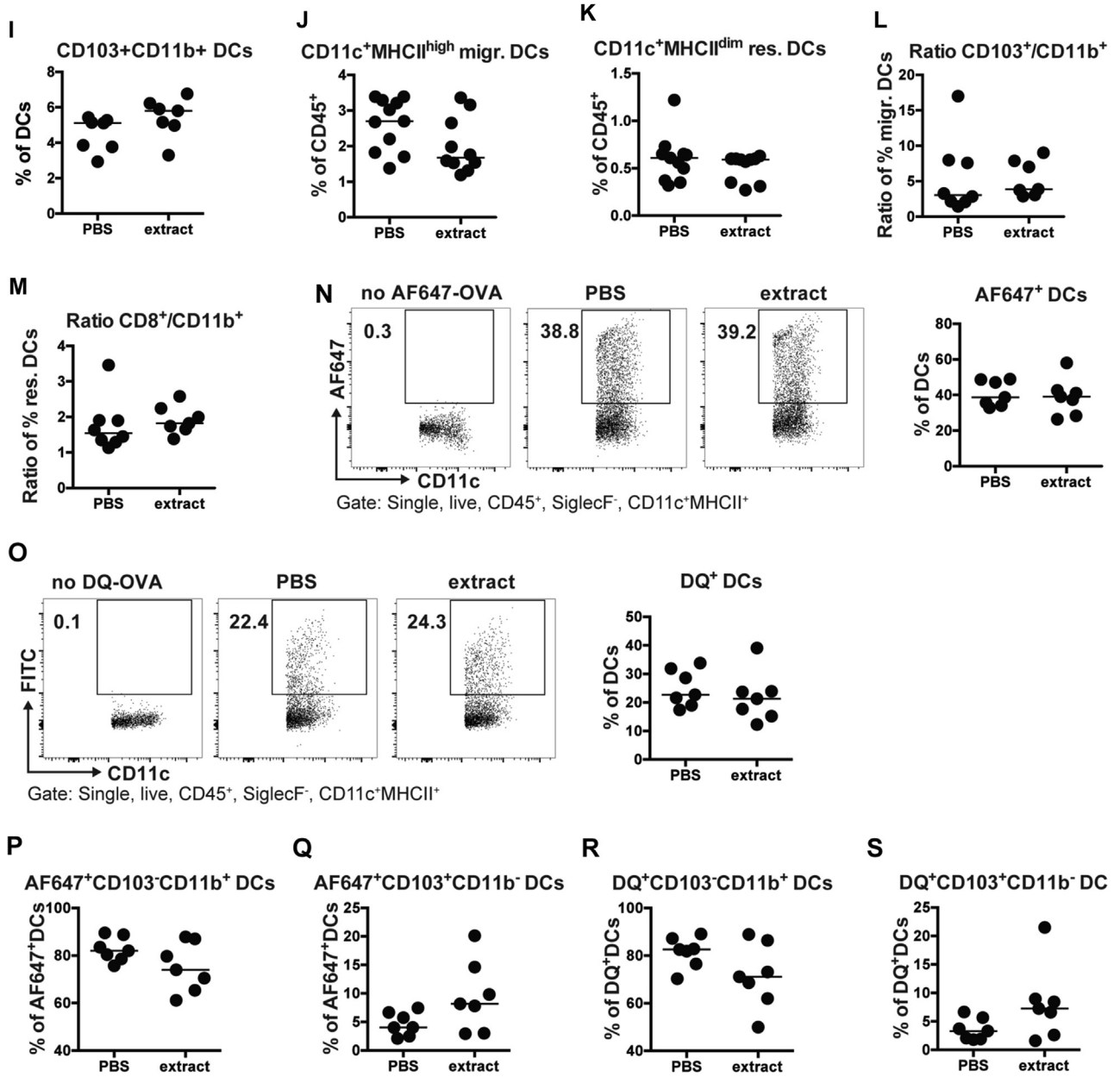
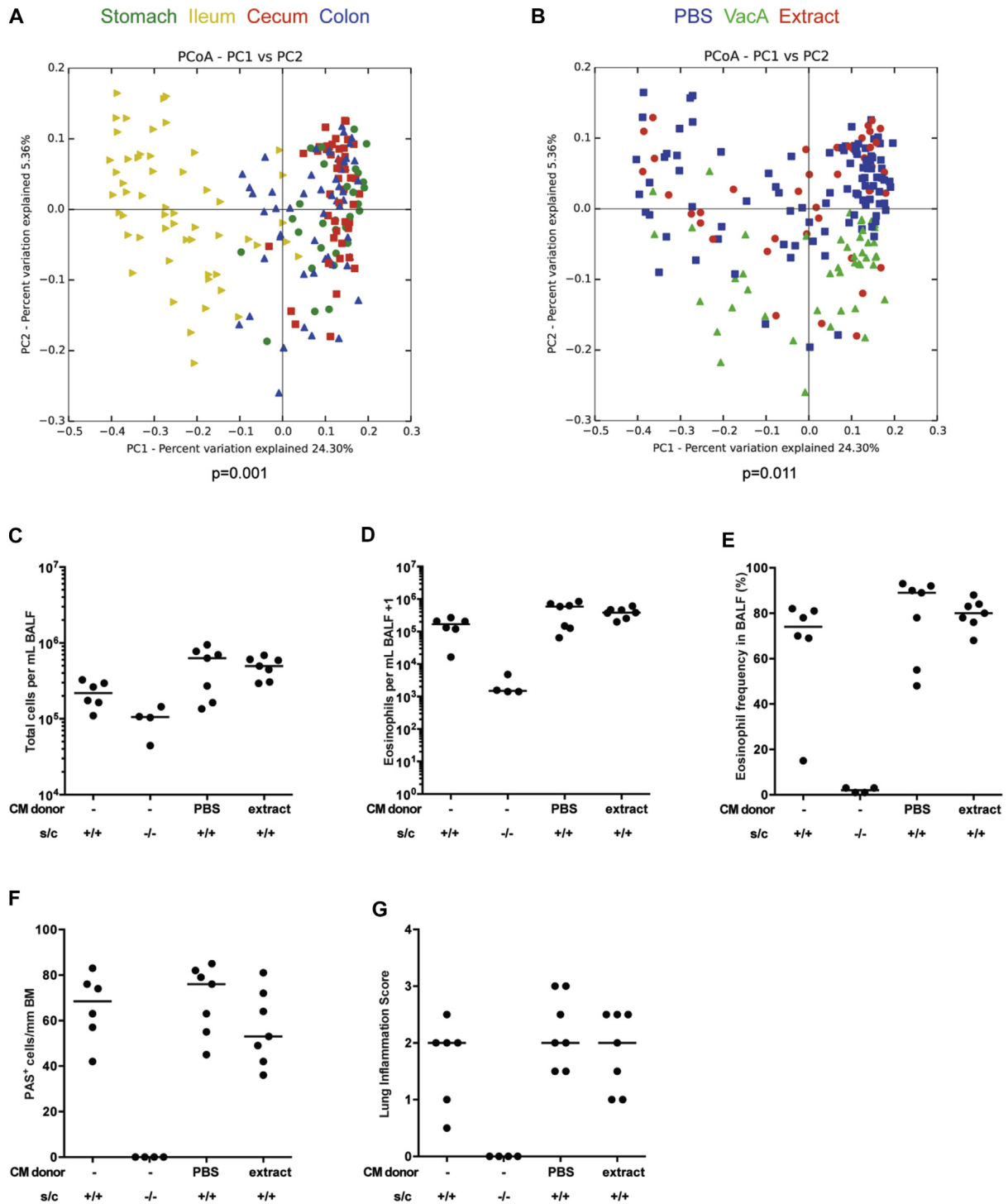
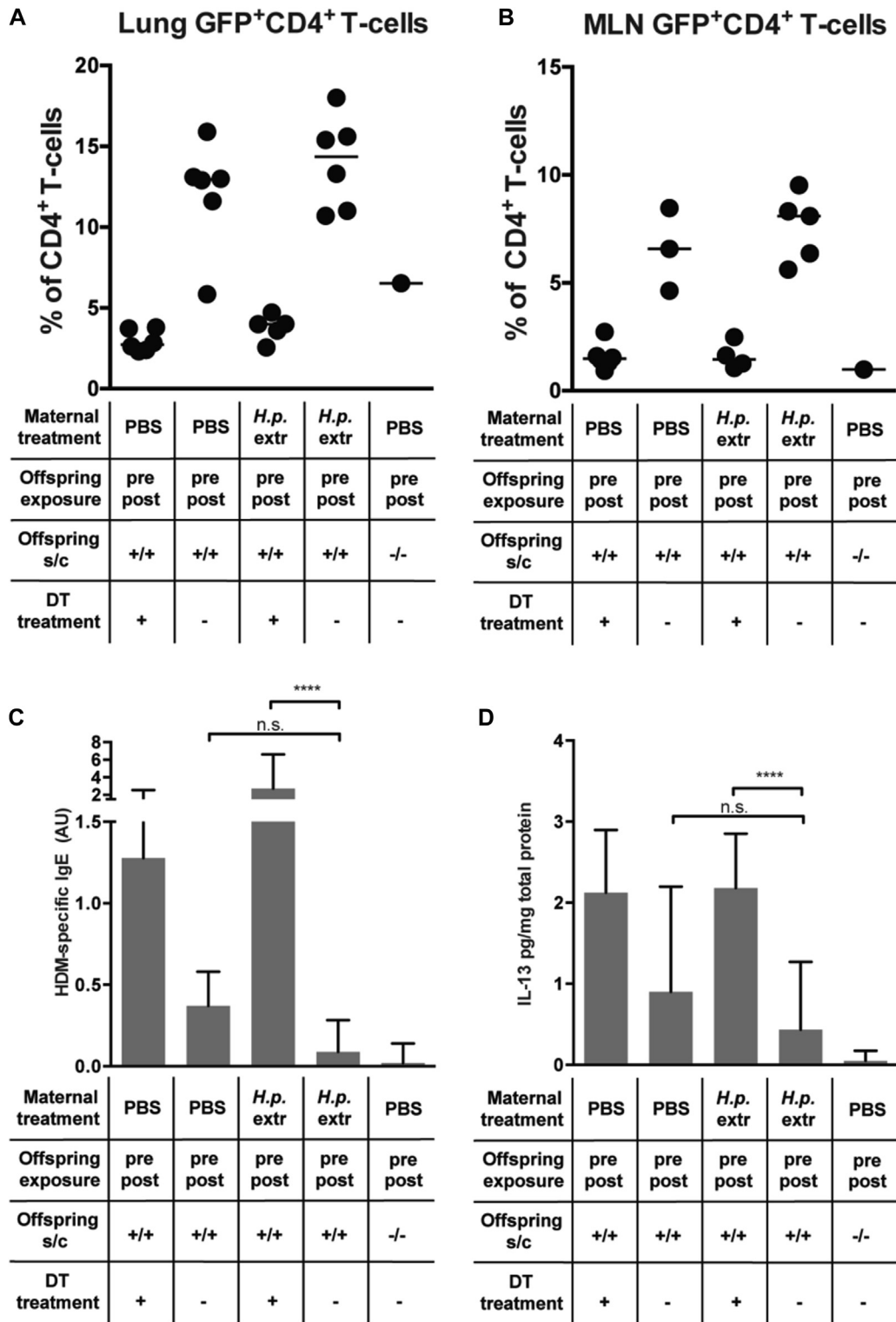


FIG E3. (Continued).



**FIG E4.** Perinatal transmaternal exposure to *H pylori* extract or VacA induces changes in the microbiota that do not confer protection against allergic airway inflammation on cecal microbiota transfer. **A** and **B**, Mice were perinatally and postnatally exposed to *H pylori* extract, VacA, or PBS through twice-weekly oral treatment of dams during pregnancy and lactation. Gastric, ileal, cecal, and colonic tissue was collected at necropsy and subjected to DNA extraction. The V4 region of the bacterial 16S rRNA gene was amplified and sequenced on the Illumina MiSeq platform. Unweighted UniFrac distances were shown in a principal coordinate (PC) analysis (PCoA) plot, where samples were rarefied at 2000 reads for all the organs assessed (Fig E4, A) and for all the treatments tested (Fig E4, B). The Adonis test was used to compare community structures between all treatment groups at both sites. **C-G**, The cecal microbiota (CM) of *H pylori* extract-exposed or PBS-exposed adult donor mice was isolated and transferred into neonates. At 6 weeks of age, recipients were sensitized and challenged (s/c) intranasally with HDM allergen alongside mice that had not received CM. Negative controls were sensitized and challenged with PBS only. Allergic airway inflammation was assessed as described in Fig 1. **C**, Total leukocytes in 1 mL of bronchoalveolar lavage fluid (BALF). **D**, Total eosinophils in 1 mL of BALF. **E**, Eosinophil frequencies in BALF. **F** and **G**, Pulmonary inflammation and goblet cell metaplasia, as assessed on stained lung sections. Results in Fig E4, C-G, are from 1 experiment. Horizontal lines indicate medians.



**FIG E5.** Depletion of Treg cells during HDM challenge abrogates allergy protection induced by perinatal transmaternal exposure to *H pylori* extract. Foxp3<sup>DTR</sup> mice were prenatally and postnatally exposed to *H pylori* extract or PBS through twice-weekly oral treatment of the dams during pregnancy and lactation, as described in Fig 5. At 6 weeks of age, offspring were sensitized and challenged (*s/c*) intranasally with HDM allergen. Negative controls were sensitized and challenged with PBS only. Where indicated, mice received a total of 4 doses (spread across 8 days) of 1  $\mu$ g of DT just before and during HDM challenge. Treg cell depletion efficiency was assessed in pulmonary leukocyte preparations, as well as MLNs, and serum HDM-specific IgE levels, as well as pulmonary IL-13 production, were quantified by means of ELISA. **A** and **B**, Treg cell depletion efficiency in the lungs (Fig E5, **A**) and MLNs (Fig E5, **B**), as assessed by using FACS of GFP<sup>+</sup> (Foxp3<sup>+</sup>) CD4<sup>+</sup> T cells at death (ie, 3 days after the last dose of DT). Note that not all MLNs could be analyzed because of technical reasons. *Horizontal lines* indicate medians. Data are from 1 of 3 representative experiments. **C** and **D**, HDM-specific IgE levels in serum and IL-13 concentrations in lung homogenates, as determined by using ELISA. *Bars* represent medians with interquartile ranges. Data in Fig E5, **C** and **D**, are pooled from 2 independent experiments. ANOVA with Dunn multiple comparison correction was used for calculation of *P* values. \*\*\*\**P* < .0001. *n.s.*, Not significant.

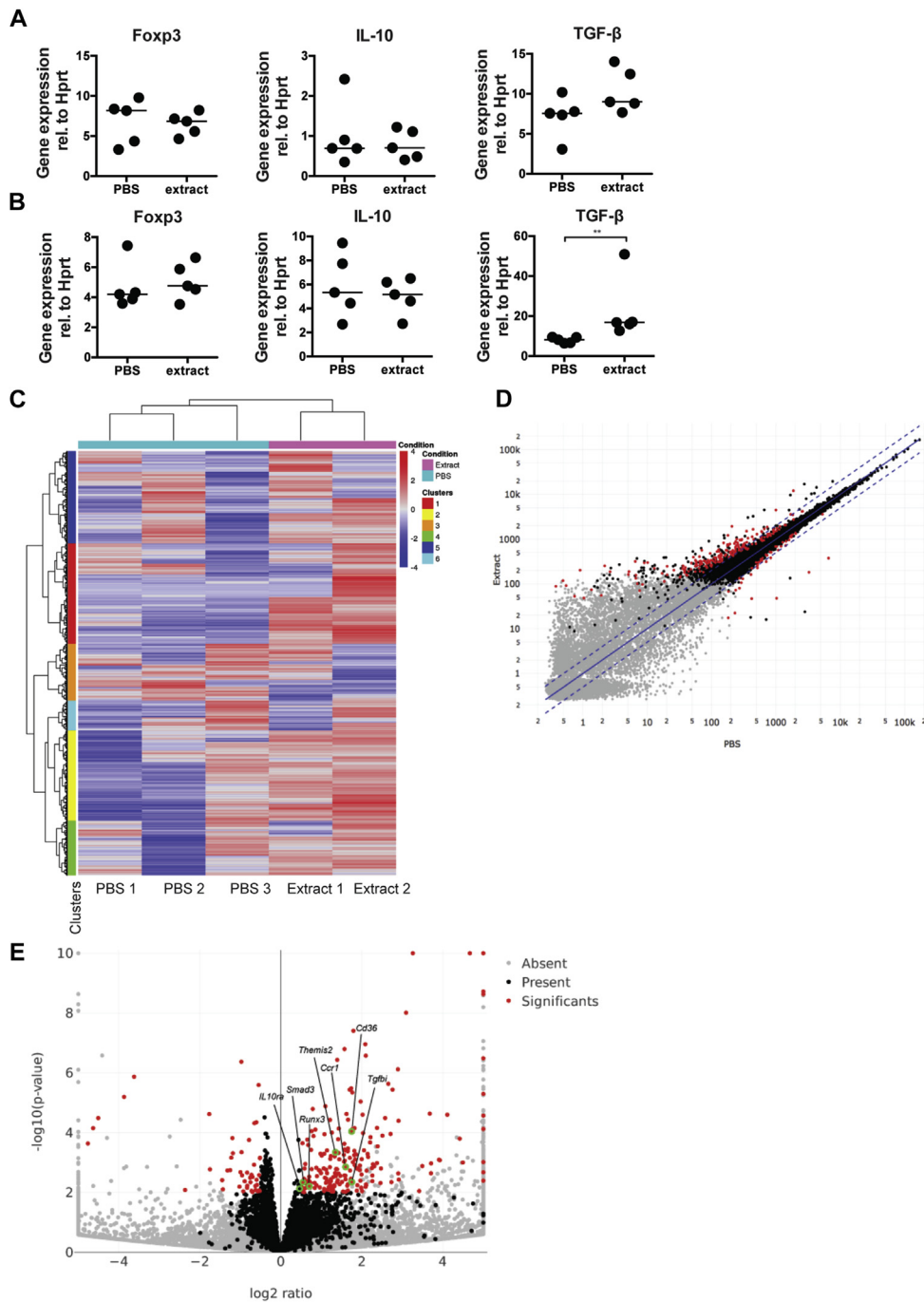


**FIG E6.** Gene expression profiling of FACS-sorted Treg cells. **A** and **B**, *Foxp3*<sup>eGFP-DTR</sup> mice were prenatally and postnatally exposed to *H pylori* extract through twice-weekly oral treatments of the dams during pregnancy and lactation. CD4<sup>+</sup>GFP<sup>+</sup> Treg cells were sorted from pulmonary leukocyte preparations (Fig E6, **A**) or MLN single-cell preparations (Fig E6, **B**) and subjected to RNA isolation and quantitative RT-PCR for *Hprt*, *Foxp3*, *Tgfb*, and *Ii10*. Samples were run on a LightCycler 480, and expression was normalized to the housekeeping gene *Hprt*. Each symbol represents 1 mouse. Data are from 1 experiment. Horizontal lines indicate medians; an unpaired Mann-Whitney *U* test was used for calculation of *P* values. \*\**P* < .01. **C-E**, Pulmonary Treg cells were sorted, as described above, and subjected to RNA isolation and sequencing on an Illumina HiSeq 2500 instrument. Samples were pooled from 3 to 4 mice, which produced yields of approximately 20,000 greater than 95% pure CD4<sup>+</sup>GFP<sup>+</sup> Treg cells per pool. Two pools of extract-treated and 3 pools of control Treg cells were sequenced. RNA sequencing reads were quality checked, mapped to the GRCm38 mouse reference genome by using STAR, and counted according to Ensembl gene annotation by using the featureCounts function in the Rsubread Bioconductor package. The EdgeR package was used to conduct statistical analysis of differential gene expression. The heat map in Fig E6, **C**, shows the result of unsupervised clustering of genes and samples by using the top 2000 most differentially expressed genes, which segregates pulmonary Treg cells from extract- and PBS-treated mice. Fig E6, **D**, shows the average expression of genes of Treg cells from extract- and PBS-treated mice; the 248 significantly different transcripts (*P* < .01) are shown in red. Note that the majority of transcripts are upregulated as a consequence of extract exposure. Fig E6, **E**, shows the same results as in Fig E6, **D**, in a volcano plot representation; select Treg cell-specific genes are annotated.

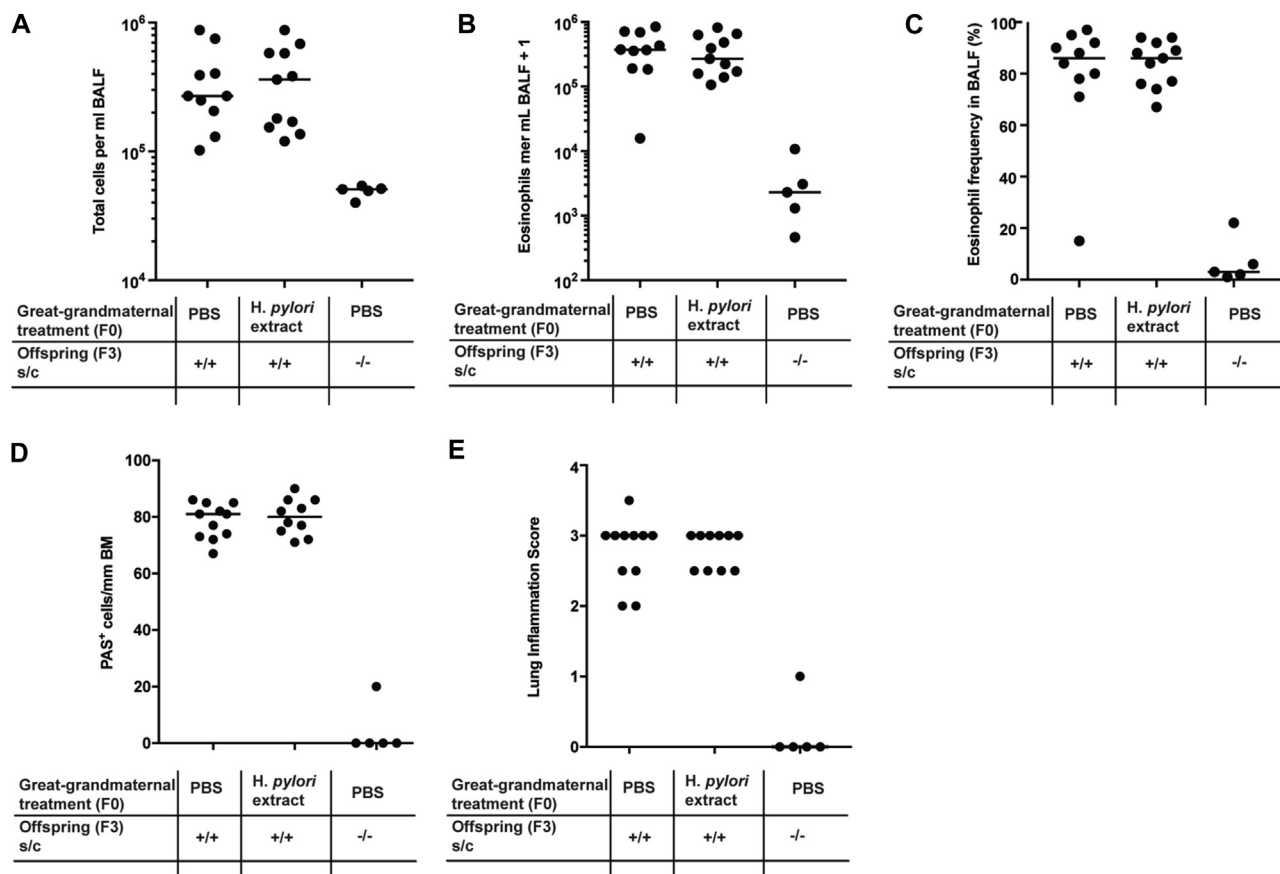


**FIG E7.** *H. pylori* extract does not reduce allergic airway inflammation in F3 offspring. F0 dams were subjected to twice-weekly oral gavage with *H. pylori* extract (*H.p. extr*) or PBS during pregnancy and lactation. Perinatally exposed F1 animals obtained in this manner were bred with each other. F2 offspring were subsequently interbred once more to obtain F3 progeny. At 6 weeks of age, F3 progeny were sensitized and challenged (*s/c*) intranasally with HDM allergen. Negative control mice were sensitized and challenged with PBS only. **A**, Total leukocytes in 1 mL of bronchoalveolar lavage fluid (*BALF*). **B**, Total eosinophils in 1 mL of *BALF*. **C**, Eosinophil frequencies in *BALF*. **D** and **E**, Pulmonary inflammation and goblet cell metaplasia, as assessed on stained lung sections. Each symbol represents 1 mouse. Results from 2 independent experiments were pooled. Horizontal lines indicate medians.